Deutsches Zentrum
für Luft- und Raumfahrt e.V.
in der Helmholtz-Gemeinschaft

# EnMAP Ground Segment

## Mission Quarterly Report #03

## 01.01.2023 to 31.03.2023

*Restriction: public*

| | |
|---|---|
| Doc. ID | EN-GS-RPT-1103 |
| Issue | 1.0 |
| Date | 21.05.2023 |

Configuration Controlled: Yes

German Remote Sensing Data Center (DFD)
Remote Sensing Technology Institute (IMF)
German Space Operations Center (GSOC)
German Research Centre for Geosciences (GFZ-Potsdam)
German Space Agency at DLR

## TABLE OF SIGNATURES

| | | |
|---|---|---|
| **Prepared** | Emiliano Carmona — Digitally signed by Emiliano Carmona<br>DN: C=DE, CN=Emiliano Carmona, E=Emiliano.Carmona@dlr.de<br>Reason:<br>Location:<br>Date: 2023.06.16 15:28:08+02'00'<br>Foxit PDF Reader Version: 12.1.2 | |
| | Date | Emiliano Carmona, (DLR MF-PBA, EnMAP OMM 01.03.2023-31.03.2023) |
| | Tobias Storch — Digital signiert von Tobias Storch<br>DN: OU=DLR MF-PBA, CN=Tobias Storch, E=tobias.storch@dlr.de<br>Grund:<br>Ort:<br>Datum: 2023.06.16 16:45:21+02'00'<br>Foxit PDF Editor Version: 12.1.2 | |
| | Date | Tobias Storch, (DLR MF-PBA, EnMAP OMM 01.01.2023-28.02.2023) |
| | Sabine Chabrillat — Digital unterschrieben von Sabine Chabrillat<br>Datum: 2023.06.19 15:04:10 +02'00' | |
| | Date | Sabine Chabrillat, (GFZ-Potsdam, EnMAP SciLead) |
| **Reviewed** | K.Wirth — Katrin Wirth<br>2023.06.21 13:23:19+02'00' | |
| | Date | Katrin Wirth, (DLR RB-MIB, dep. EnMAP OMM) |
| | Sabine Engelbrecht — Digital signiert von Sabine Engelbrecht<br>DN: C=DE, S=Nordrhein-Westfalen, L=Koeln, O=Deutsches Zentrum fuer Luft- und Raumfahrt e.V. (DLR), SN=Engelbrecht, G=Sabine, CN=Sabine Engelbrecht<br>Grund: Ich habe dieses Dokument geprüft<br>Ort: Oberpfaffenhofen<br>Datum: 2023.06.19 16:49:31+02'00'<br>Foxit PDF Editor Version: 12.1.2 | |
| | Date | Sabine Engelbrecht, (DLR DFD-INF, EOC PAD) |
| | R. Größel — Robert Größel<br>2023.06.20 11:26:05+02'00' | |
| | Date | Johannes Greulich, (DLR RB-MIB, GSOC PAD) |
| | Karl Segl — Digital unterschrieben von Karl Segl<br>Datum: 2023.06.23 14:45:25 +02'00' | |
| | Date | Karl Segl, (GFZ-Potsdam, dep. EnMAP SciLead) |
| **Approved & Released** | i.A. S. Fischer — Digital signiert von Sebastian Fischer<br>Datum: 2023.06.23<br>14:52:24<br>+02'00' | |
| | Date | Sebastian Fischer, (DLR AR-AO, EnMAP MM) |

## DISTRIBUTION LIST

The document is publicly available via www.enmap.org.

# CHANGE RECORD

| Version | Date | Chapter | Comment |
|---|---|---|---|
| 1.0 | 21.05.2023 | All | First issue of Mission Quarterly Report #03 |

Custodian of this document is Carmona, Emiliano.

# CONTENTS

## LIST OF FIGURES

# LIST OF TABLES

# 1. Introduction

## 1.1 Purpose

This mission quarterly report (MQR) states information on the EnMAP mission status with regard to the registered user community, announcements-of-opportunities and observations as well as the status of the user interfaces, satellite (platform and payload), ground stations (S-band and X-band), processor (Archive, Level 1B, Level 1C, Level 2A (land and water)), calibration (spectral, radiometric, geometric), data quality control and validation of EnMAP.

Please visit www.enmap.org for further information on EnMAP.

## 1.2 Scope

This third Mission Quarterly Report (MQR) applies to the operations of EnMAP in the reporting period of Routine Phase (RP) from **01.01.2023 to 31.03.2023 (Q1/2023)**.

# 2. References

| Reference Identifier | Document Identifier and Title |
|---|---|
| [1] | L. Guanter et al. (2015) The EnMAP Spaceborne Imaging Spectroscopy Mission for Earth Observation. Remote Sensing, Issue 7, pp. 8830-8857. |
| [2] | EN-GS-UM-6020 Portals User Manual, Version 1.0 |
| [3] | EN-PCV-ICD-2009 Product Specification, Version 1.8 |
| [4] | EN-PCV-TN-4006 Level 1B ATBD, Version 1.7 |
| [5] | EN-PCV-TN-5006 Level 1C ATBD, Version 1.6 |
| [6] | EN-PCV-TN-6007 Level 2A (land) ATBD, Version 2.2 |
| [7] | EN-PCV-TN-6008 Level 2A (water) ATBD, Version 3.1 |
| [8] | Chabrillat, S. et al. (2022) EnMAP Science Plan. EnMAP Technical Report, DOI: 10.48440/enmap.2022.001 |
| [9] | Lachérade, S. et al. (2014) Introduction to the Sentinel-2 radiometric calibration activities during commissioning phase. Proc. SPIE, Vol. 9241, DOI: 10.1117/12.2067123 |

**Table 2-1 References**

# 3. Terms, Definitions and Abbreviations

Terms, definitions and abbreviations for EnMAP are collected in a database which is publicly accessible via Internet on www.enmap.org.

An Earth observation of swath length $n \times 30$ km (and swath width 30 km) is separated into $n$ tiles of size 30 km × 30 km.

# 4. Mission

## 4.1 Mission Objectives

The primary goal of EnMAP (Environmental Mapping and Analysis Program) is to measure, derive and analyze quantitative diagnostic parameters describing key processes on the Earth's surface [1].

During the mission operations, with the successful launch on 1st of April 2022 and an expected operational mission lifetime of at least 5 years, EnMAP will provide valuable information for various application fields comprising soil and geology, agriculture, forestry, urban areas, aquatic systems, ecosystem transitions.

## 4.2 Mission Description

The major elements of the EnMAP mission are the EnMAP Space Segment, built by OHB System AG and owned by the German Space Agency at DLR, the EnMAP Ground Segment built and operated by DLR institutes DFD, MF, RB, and the EnMAP User and Science Segment represented by GFZ. The project management of the EnMAP mission is responsibility of the German Space Agency at DLR.

The EnMAP Space Segment is composed of

- the platform providing power and thermal stability, orbit and attitude control, memory, S-band uplink/downlink for TM/TC data transmission/reception, X-band downlink for payload data transmission, and
- the payload realized as a pushbroom imaging dual-spectrometer covering the wavelength range between 420 nm and 2450 nm with a nominal spectral resolution ≤ 10 nm and allows in combination with a high radiometric resolution and stability to measure subtle reflectance changes.

The EnMAP satellite is operated on a sun-synchronous repeat orbit to observe any location on the globe with comparable illumination conditions. This allows a maximum reflected solar input radiance at the sensor with an acceptable risk for cloud coverage.

The EnMAP Ground Segment is the interface between Space Segment and User and Science Segment. It comprises functionalities to

- perform planning of imaging, communication and orbit maneuver operations, provision of orbit and attitude data, command and control of the satellite, ground station networks (in particular: Weilheim, Germany, for S-band and Neustrelitz, Germany, for X-Band), receive satellite data, perform long-term archiving and delivery of products, and
- perform processing chain (for systematic and radiometric correction, orthorectification, atmospheric compensation), instrument calibration operations, and the data quality control of the products.

The EnMAP mission interfaces to the international science and user community through the EnMAP Portal www.enmap.org with official information related to EnMAP by DLR and GFZ-Potsdam (as the document in hand) and links for ordering observations and products.

The EnMAP Science Segment is represented by the EnMAP Science Advisory Group chaired by the mission principal investigator at the GFZ-Potsdam. The Science Segment addresses aspects such as

- supporting and performing validation activities to improve sensor performance and product quality
- developing scientific and application research to fully exploit the scientific potential of EnMAP [8] including provision of software tools for EnMAP data processing and analyses (EnMAP-Box) and provision of teaching and education materials (HYPERedu)
- Organizing workshops, summer schools and in general information, training and networking activities for the user community

The EnMAP User Segment is the community of German and international users ordering acquisitions and accessing products of EnMAP.

## 4.3 Mission Status Summary

The mission entered its routine phase (RP) on 02.11.2022. On 13.12.2022 an instrument anomaly occurred and Earth observations, as well as Calibrations measurements, could not be performed until the instrument software was patched in February 2023. On 13.02.2023 the instrument anomaly was fully recovered with no limitations of functionality and not requiring the use of redundancies. With the exception of anomalies on 27.02.2023 and 20.03.2023 resolved with a reset of onboard data science storage, the instrument has been operating normally since 13.02.2023.

661 Earth observations of 30 km swath width and up to 990 km swath length were successfully performed between 01.01.2023 and 31.03.2023 which resulted in 5183 archived Earth observation tiles of 30 km × 30 km. In total, 3463 Earth observations were performed until 31.03.2023 by the EnMAP team (mostly during commissioning phase) and the 805 registered Science users which resulted in 22181 archived Earth observation tiles and 20133 Earth observation tiles delivered to users. Details are presented in Sections 5 and 6.

The following limitations are applicable at 31.03.2023:

- Instrument Anomaly and recovery of operations (see above)
- Continuous degradation of the VNIR sensor is observed and addressed with monthly adjustments of the radiometric calibration. The rate of degradation has kept decreasing and at the time of the reporting period is practically negligible in most bands. Radiometric requirements are expected to remain within specifications between calibrations.
- Some striping effects in SWIR data in the along-track direction more visible in uniform areas with a strong spectral gradient.
- Limitations on user interfaces are expected to be solved by the end of Q2/2023 as detailed in section 7.1 [2].
- Implementation of auxiliary instrument data (VC-AUX) in archived L0 data products not completed yet.

The following changes where implemented in the reporting period:

- To avoid leaps in consecutive radiometric calibration coefficients, due to the degradation of the VNIR sensor, modifications in the radiometric calibration and radiometric correction processor were introduced in processor version 01.02.00.
- Further improvements to the radiometric correction processor for mitigating the across-track striping effects were introduced in processor version 01.02.00.
- Improvements in geometric VNIR-SWIR co-registration were introduced with a new geometric calibration table and software updates introduced in version 01.02.00.
- Several improvements on user interfaces introduced during Q1/2023 (see section 7.1).

The following changes are expected to be performed until 30.06.2023 and later:

- Further improvements on archived products, e.g. on VNIR-SWIR co-registration, quicklooks and quality attributes, are expected by a re-processing planned to start in June 2023.
- Correction of problem with speed of light correction in L1C processor to reduce RMS Error of geolocation accuracy in the Y direction
- For changes concerning the User Interfaces see chapter 7.1
- Correction of radiometric striping in the along-track direction (see chapter 7.6.2.3, point 3)

# 5. Users and Announcements-of-Opportunities

## 5.1 Users

| Country/*Continent (No of Countries)* | 02.11.2022 to 31.12.2022 | 01.01.2023 to 31.03.2023 | 02.11.2022 to 31.03.2023 |
|---|---|---|---|
| *Europe (31)* | 442 | 248 | 690 |
| • Germany | 228 | 110 | 338 |
| • Italy | 38 | 20 | 58 |
| • France | 25 | 15 | 40 |
| • Great Britain | 26 | 11 | 37 |
| • Spain | 24 | 8 | 32 |
| • Netherlands | 13 | 8 | 21 |
| • Portugal | 12 | 5 | 17 |
| • Turkey | 14 | 6 | 20 |
| • Greece | 8 | 9 | 17 |
| • Belgium | 5 | 8 | 13 |
| • Poland | 7 | 8 | 15 |
| • Others | 42 | 40 | 82 |
| *North America (2)* | 79 | 55 | 134 |
| *South America (13)* | 49 | 25 | 74 |
| *Asia (13)* | 81 | 49 | 130 |
| *Africa (16)* | 41 | 29 | 70 |
| *Australia + New Zealand (2)* | 23 | 11 | 34 |
| *Total* | 726 | 418 | 1144 |
| *Rejected** | 1 | 1 | 2 |

**Table 5-1 Number of registered users per continent**

*Users are rejected because of, e.g. EU sanction list checks, data policy or license violations.

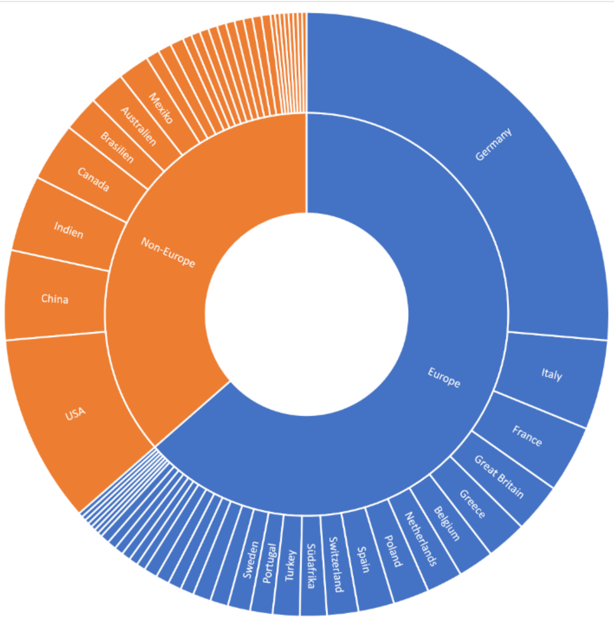


01.01.2023 to 31.03.2023 with total 418 Users of 61 different countries.

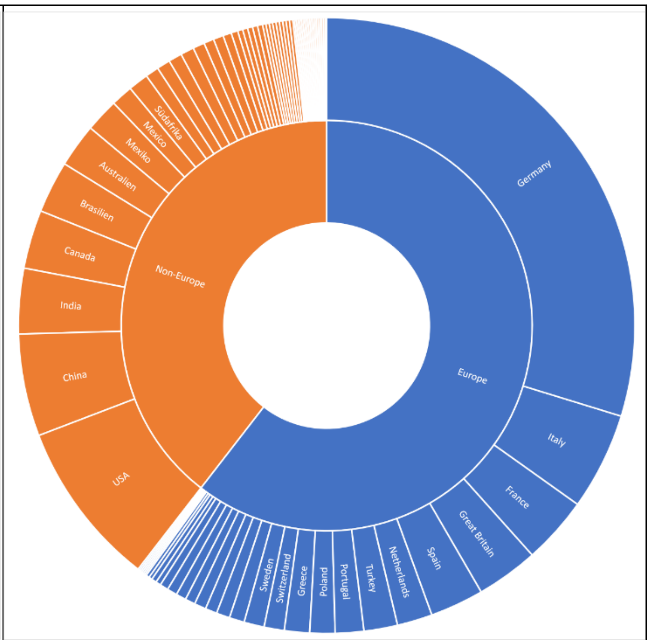


02.11.2022 to 31.03.2023 with total of 1144 Users of 81 different countries.

**Figure 5-1 Number of registered users per country**

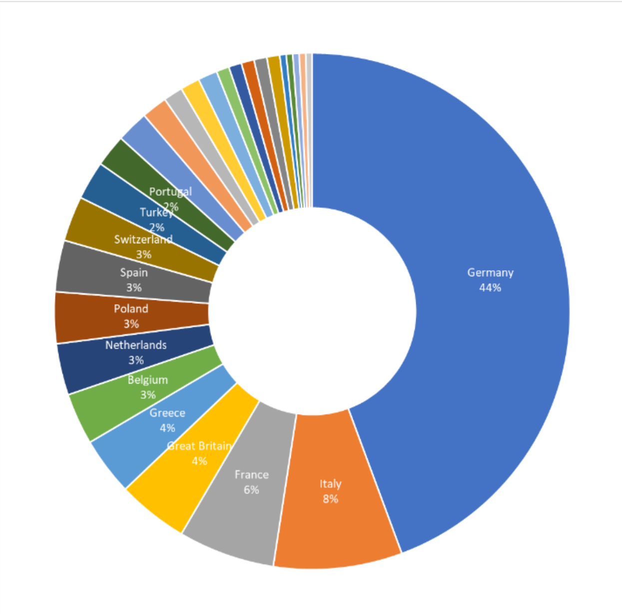


01.01.2023 to 31.03.2023 with total of 248 European Users of 27 different countries.

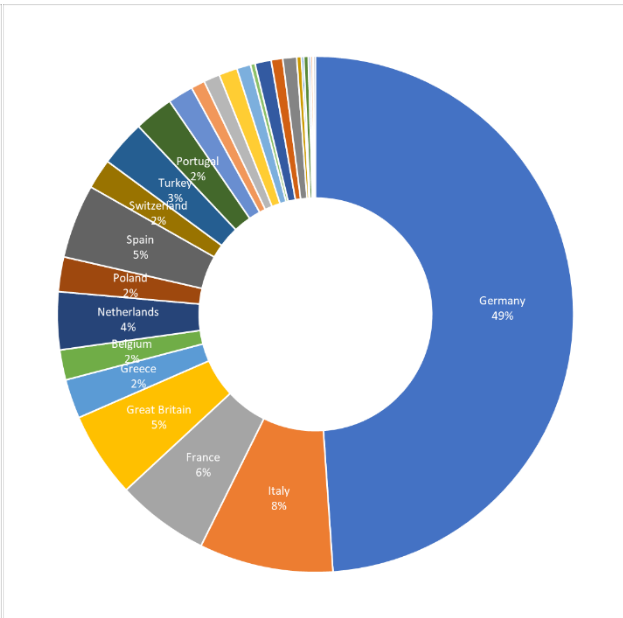


02.11.2022 to 31.03.2023 with total of 690 European Users of 31 different countries.

**Figure 5-2 Number of registered users per European country**

Registered users belong to different categories, therefore e.g. All/World ≠ Science/World + Others/World.

| User per Category | | 02.11.2022 to 31.12.2022 | 01.01.2023 to 31.03.2023 | 02.11.2022 to 31.03.2023 |
|---|---|---|---|---|
| Cat-1 Science | Total | 480 | 325 | 805 |
| | AO Process 00001 | 327 | 232 | 559 |
| | AO Process 00002 | 239 | 186 | 425 |
| Cat-1 Distributor | Total | 323 | 223 | 546 |
| Rejected | | 1 | 1 | 2 |

**Table 5-2 Number of registered users per category (Cat-1 Science and Cat-1 Distributor)**

## 5.2 Announcements-of-Opportunities

| Announcement-of-Opportunity | 02.11.2022 to 31.12.2022 | | 01.01.2023 to 31.03.2023 | | 02.11.2022 to 31.03.2023 | |
|---|---|---|---|---|---|---|
| | Proposals | Total tiles | Proposals | Total tiles | Proposals | Total tiles |
| AO#1 | 33 | 2774 | 78 | 5302 | 111 | 8076 |
| AO#2 | 20 | 2288 | 47 | 13220 | 67 | 15508 |
| Total | 53 | 5062 | 125 | 18522 | 178 | 23584 |

**Table 5-3 Number of released science proposals to Announcement-of-Opportunity**

| Icon | Topic | 02.11.2022 to 31.12.2022 | | 01.01.2023 to 31.03.2023 | | 02.11.2022 to 31.03.2023 | |
|---|---|---|---|---|---|---|---|
| | | Proposals | Total Tiles | Proposal | Total Tiles | Proposal | Total Tiles |
| | VEGETATION | 18 | 2207 | 60 | 11555 | 78 | 13762 |
| | GEO/SOIL | 15 | 442 | 37 | 2263 | 52 | 2705 |
| | WATER | 9 | 868 | 12 | 549 | 21 | 1417 |
| | SNOW/ICE | 0 | 0 | 4 | 1190 | 4 | 1190 |
| | URBAN | 0 | 0 | 2 | 256 | 2 | 256 |
| | ATMOSPHERE | 3 | 385 | 1 | 204 | 4 | 589 |
| | HAZARD/RISK | 1 | 0 | 2 | 39 | 3 | 39 |
| | METHODS | 1 | 120 | 4 | 466 | 5 | 586 |
| | CAL/VAL | 6 | 1040 | 4 | 2000 | 10 | 3040 |

| Icon | Topic | 02.11.2022 to 31.12.2022 | | 01.01.2023 to 31.03.2023 | | 02.11.2022 to 31.03.2023 | |
|---|---|---|---|---|---|---|---|
| | | Proposals | Total Tiles | Proposal | Total Tiles | Proposal | Total Tiles |
| | Total | 53 | 5062 | 126 | 18522 | 179 | 23584 |

**Table 5-4 Number of accepted science proposals and total number of requested of tiles per topic**

# 6. Archived and Delivered Observations

The following table shows the number of archived Earth Observation and Calibration products and their sizes within the specified time frames.

| Type | Archived | | 01.01.2023 to 31.03.2023 | | until 31.03.2023 | |
|---|---|---|---|---|---|---|
| | | | Number Tiles / Observations | Size (in GB) | Number Tiles / Observations | Size (in GB) |
| Earth Observation (EO) | Yes | Total | 5183 / 661 | 2415.7 | 22181 / 3463 | 10346.6 |
| | | Average / Day | 57.6 / 7.3 | 26.8 | 60.8 / 9.5 | 28.3 |
| | No | Total | 257 | | 816 | |
| | | Average / Day | 2.9 | | 2.2 | |
| Calibration (CAL) | Yes | Total | 17 | 66.1 | 88 | 379.2 |
| | | Average / Day | 0.2 | 0.7 | 0.2 | 1.0 |
| | No | Total | 0 | | 1 | |
| | | Average / Day | 0 | | 0.003 | |

**Table 6-1 Number and size of archived and not archived products**

The following table shows the number of delivered products and their sizes within the specified time frames. Product deliveries result either directly from acquisition orders (Observation) and catalog orders (Archive)

| Type | Delivered | | 01.01.2023 to 31.03.2023 | | until 31.03.2023 | |
|---|---|---|---|---|---|---|
| | | | Number Tiles / Observations | Size (in GB) | Number Tiles / Observations | Size (in GB) |
| Earth Observation (EO) | Observation | Total | 2599 / 400 | 1033.7 | 20133 / 2884 | 8687.7 |
| | | Average / Day | 28.9 / 4.4 | 11.5 | 55.2 / 7.9 | 23.8 |
| | Archive | Total | 4977 | 24775.3 | 9787 | 48249.2 |
| | | Average / Day | 55.3 | 275.3 | 26.8 | 132.2 |
| Calibration (CAL) | Observation | Total | 16 | 65.3 | 66 | 307.5 |
| | | Average / Day | 0.2 | 0.7 | 0.2 | 0.8 |
| | Archive | Total | 1 | 0.8 | 68 | 3091.9 |
| | | Average / Day | 0.0 | 0.0 | 0.2 | 8.5 |

**Table 6-2 Number and size of delivered products**

## 6.1 Archived Observations

The following figures show the heatmaps for the whole world and for Europe within the specified time frames. The heatmaps represent the frequencies of products at a geographic location, where the number of products increases from blue over red to yellow and white.

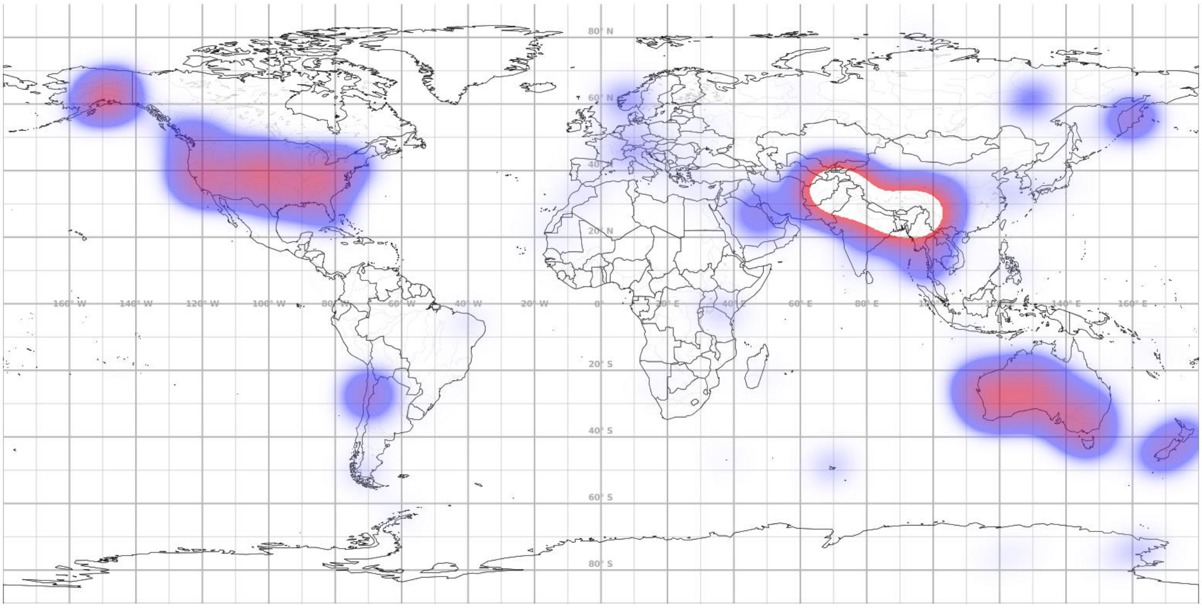

01.01.2023 to 31.03.2023 with 5183 tiles

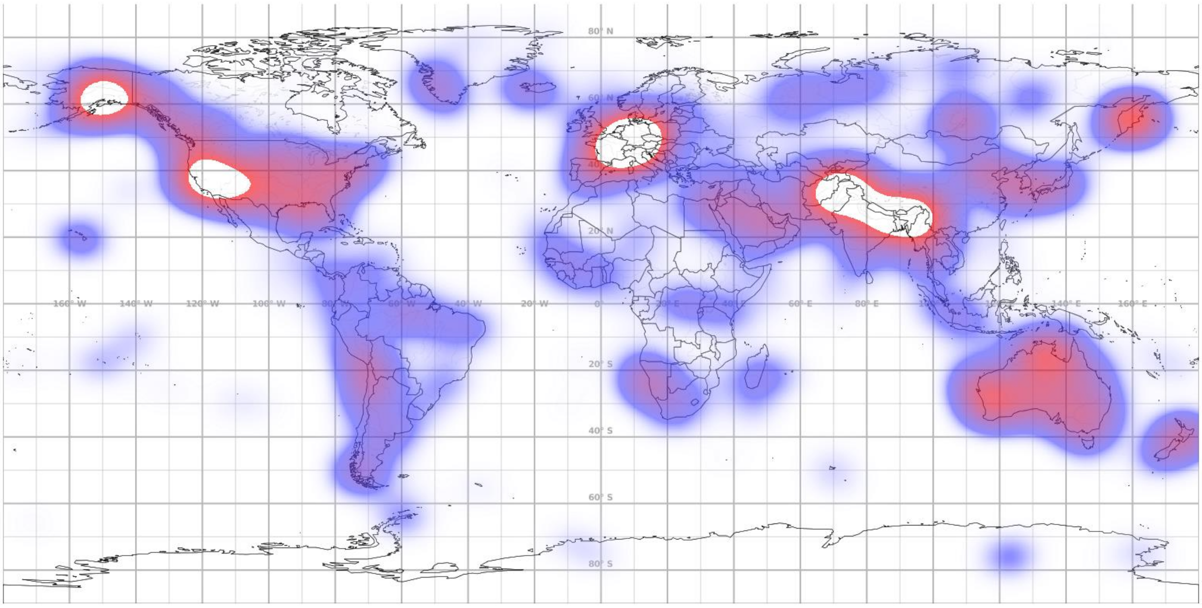

until 31.03.2023 with 22181 tiles (includes commissioning phase acquisitions)

**Figure 6-1 Geographic location of all Earth observation tiles archived, World**

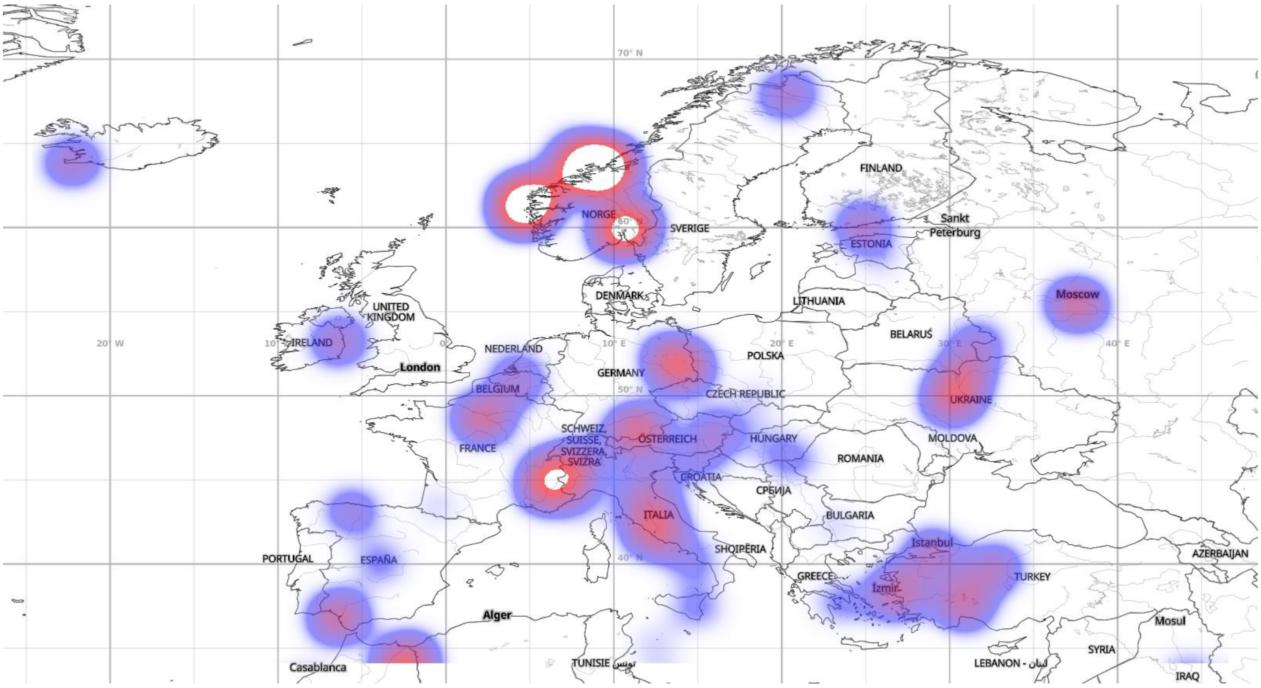


01.01.2023 to 31.03.2023 with 173 tiles

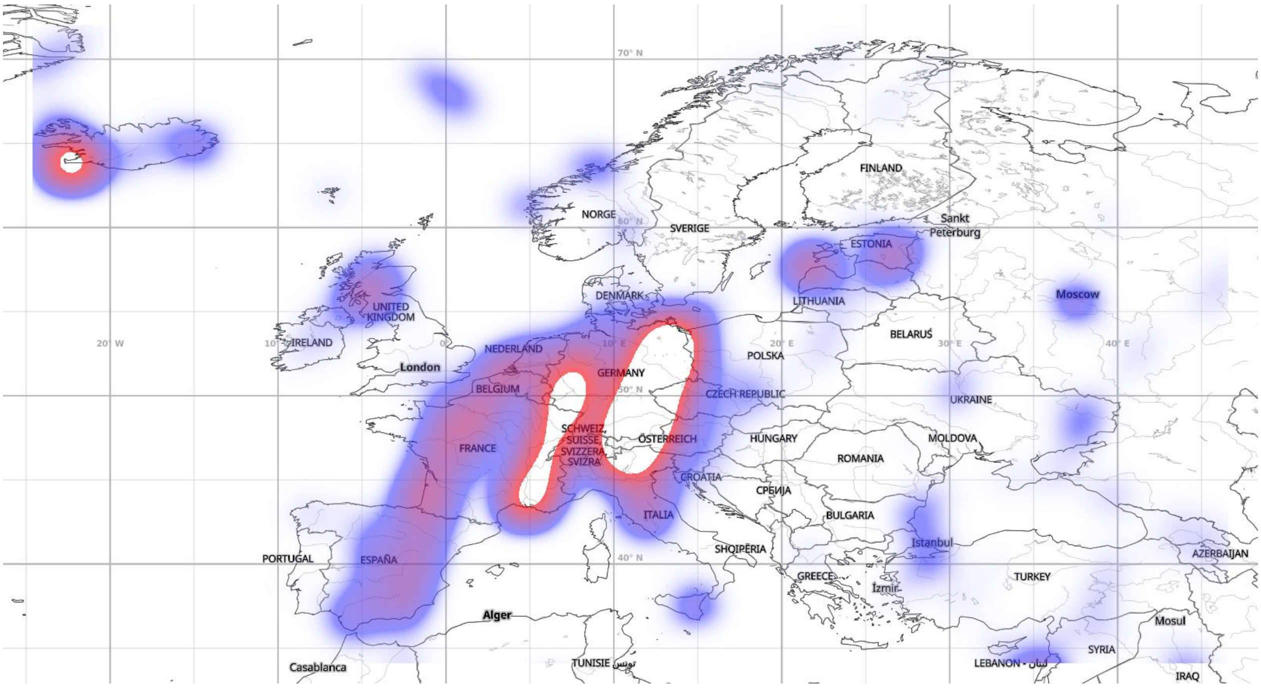


until 31.03.2023 with 2385 tiles (includes commissioning phase acquisitions)

**Figure 6-2 Geographic location of all Earth observation tiles archived, Europe**

The following figures show the distribution of cloud coverage for the archived products.

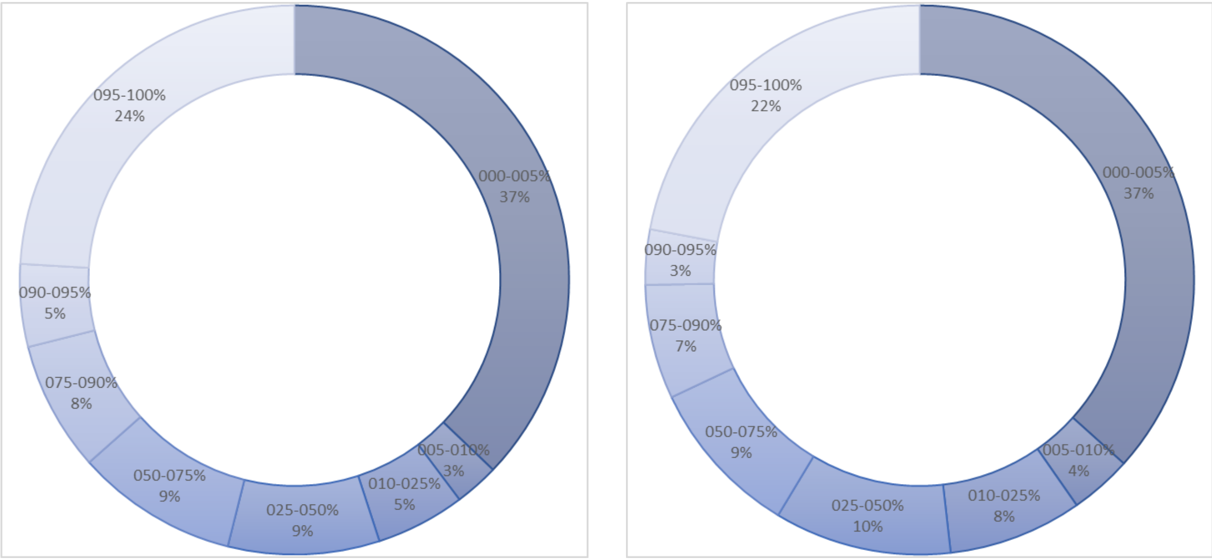


01.01.2023 to 31.03.2023 with 5183 tiles | until 31.03.2023 with 22181 tiles (includes commissioning)

**Figure 6-3 Cloud coverage in [%] of archived Earth observation tiles**

The following figures show the distribution of observation angles for the archived products.

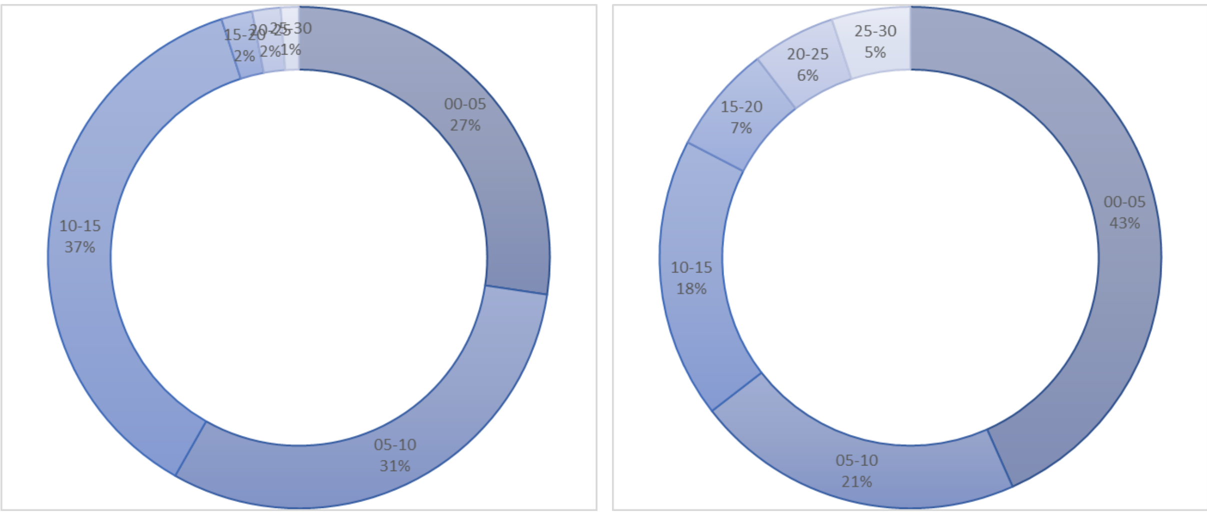


01.01.2023 to 31.03.2023 with 5183 tiles | until 31.03.2023 with 22181 tiles (includes commissioning)

**Figure 6-4 Observation angle of archived Earth observation tiles**

## 6.2 Delivered Observations

The following figures show the distribution of processing level of the delivered products from acquisition orders.

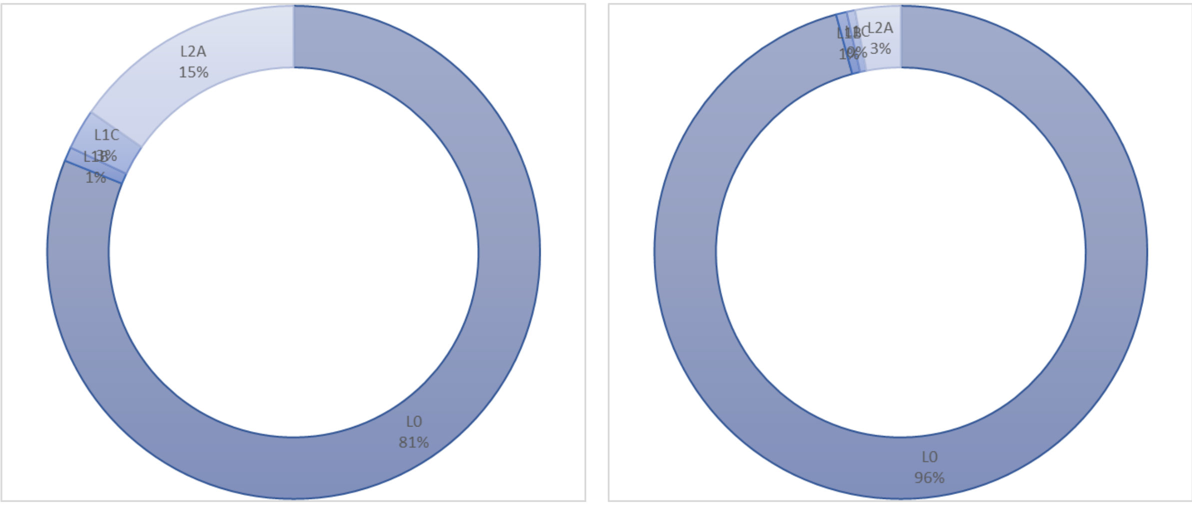


01.01.2023 to 31.03.2023 with 2599 tiles    until 31.03.2023 with 20133 tiles (includes commissioning)

**Figure 6-5 Levels of delivered Earth observation tiles from acquisition orders**

The following figures show the distribution of processing level and correction type (for L2A) of the delivered products from catalog orders.

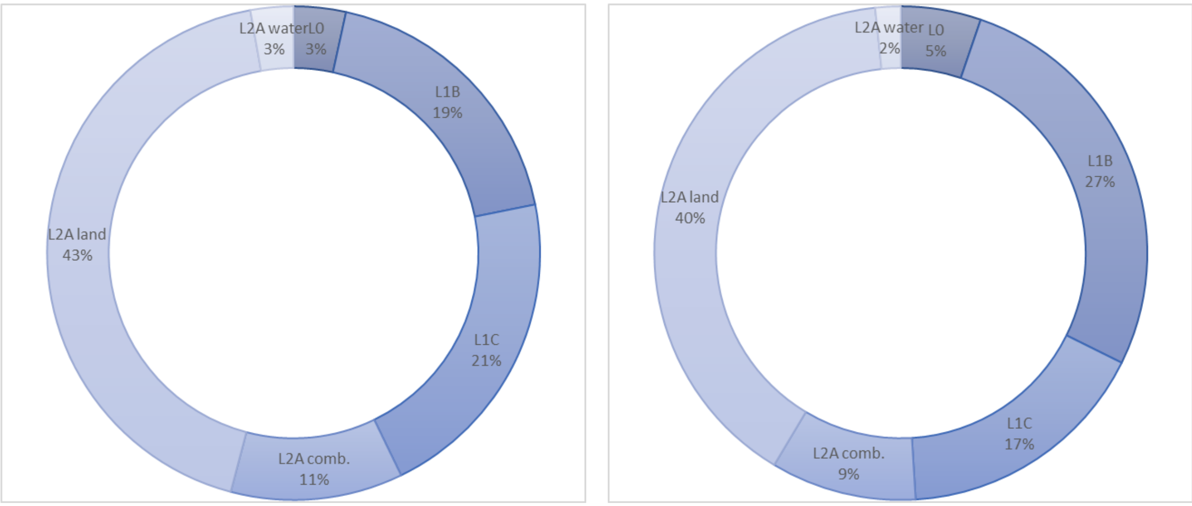


01.01.2023 to 31.03.2023 with 4977 tiles    until 31.03.2023 with 9787 tiles (includes commissioning)

**Figure 6-6 Levels of delivered Earth observation tiles from catalog orders**

# 7. Detailed Status

## 7.1 User Interfaces

The following limitations in the IPP were applicable during Q1/2023 and remain being applicable as of 31.03.2023:

- The option OR-SPC (Observation Requests based on user proposals) Area Single-pass for ordering of Earth observations by specifying dedicated single acquisitions is not yet released and will be available at end of Q2/2023. As the alternative option OR-SPC Point Multi-pass is available and fully operational that delay is not blocking for ordering of Earth observations.
- IPP Planning Support Tool: The option to submit coordinate values to support the users in ordering datatakes for precisely pre-defined geographical areas of interest is not yet released. This option will be made available to the users during Q2/2023.

On feedback of the users the following improvements of the IPP User Interface were implemented and made available to the users in Q1/2023:

- User Portal
    - In section *Personal Area* a missing attribute was added
- Proposal Portal
    - The screens for Proposal submission were enhanced by messages guiding the user through the workflow by indicating data still to be submitted, or by suggesting next steps the user can choose from to complete his/her Proposal content.
    - The screen displaying the content of a user Proposal was enhanced by mouseover info buttons explaining the meaning of the Proposal attributes.
- OR-SPC Planning Support and Ordering Portal
    - The screens for specification of Processing Options for L1C respectively L2A products were enhanced by mouseover info buttons for each of the parameters indicating the default value of that parameter.
    - Screen for specification of the acquisition-related parameters
        - Parameters being not applicable for ordering were blocked (*Preview Sunglint; Preview Clouds; Cloud Coverage Intensity Threshold*)
        - The parameter *Cloud Coverage Threshold* was enhanced by a mouseover info button explaining to the user how the value should be chosen depending on the user needs.
- OR-SPC Portal, User Orders
    - For OR-SPC orders the option was added to retrieve the datatake coverage and to display it on a map (equivalent to the display of the datatake coverage in the Planning Support Tool).

The following changes are expected to be performed until 30.06.2023 and later

- See limitations listed above
- IPP is to be extended to support Application Support in the approval of Cat-2 role requests (Cat-2 role is currently inhibited).
- OR-SPC Planning Support: Parameter *Path Direction* requires an Info Button explaining its usage to the user.
- AO Processes are to be assigned two Date Ranges (for Proposal submission; for datatake ordering) defining rules for Cat-1 Users:
  - IPP Proposal Portal / AO Screen: to be enhanced to support the specification of those date ranges by the PI-AO;
  - IPP Proposal Portal / Proposals submission: to be enhanced to ensure that the date range for Proposal submission is kept by the Cat-1 User;
  - IPP OR-SPC Planning Support Portal: to be enhanced to ensure that the date range for datatake ordering for a Proposal is kept by the Cat-1 User.

Further improvements to the user interfaces based on user feedback are continuously on-going.

## 7.2 Satellite

From 13.02.2023 an instrument outage was required due to an anomaly as detailed in Section 4.3.

### 7.2.1 Orbit

The reference orbit is a Sun-synchronous polar orbit with a mean local time of descending node of 11:00 hrs and a repeat cycle of 398 revolutions in 27 days at an altitude of 643 km (lateral deviation of at most 22 km at equator and altitude deviation of at most 6 km).

During 2023 Q1, a total of two in-plane and five out-of-plane orbit maneuvers were executed. The resulting performance error was estimated by Flight Dynamics to be between 0.1 % and 1.3 %. No collision avoidance maneuver was required in this quarter. Both Orbit Control System (OCS) thrusters were actuated a total of seven times during the above-mentioned orbit maneuvers. No actuations of the Ball Latch Valve or other OCS configuration changes were performed during 2023 Q1.

### 7.2.2 Life Limited Items

| Life-Limited Item | 01.01.2023 to 31.03.2023 | until 31.03.2023 | until end-of-life |
|---|---|---|---|
| Fuel | +1.0 kg | 3.9 kg | >15 years |
| Battery and Solar Cells | nominal | nominal | nominal |
| Shutter Usage | +0.8 % | 3.9 % | 19.6 years (@ daily use) |
| FAD movements | +2.0 % | 11.0 % | 8.3 years (@ monthly use) |
| Diffusor Exposure | +4.0 % | 21.4% | 5.1 years (@ monthly use) |
| On-Board Calibration Equipment Usage | | | |
| - OBCA SPC lamp 1 | +0.8 % | 4.2 % | 20.2 years (@ biweekly use) |
| - OBCA RAD lamp 1/LED 1 | +1.8 % | 7.3 % | 7.8 years (@ weekly use) |
| - FPA LEDs 1 | +0.3 % | 2.4 % | 44 years (@ monthly use) |

**Table 7-1 Status of life-limited items**

### 7.2.3 Redundancies

To date, the SWIR wavelength range is covered by SWIR-A (SWIR-B can be activated using a one-time switch mechanism).

All satellite subsystems are using nominal configurations.

## 7.3 Ground Stations

### 7.3.1 S-Band

| S-Band Ground Stations | 01.01.2023 to 31.03.2023 | | |
|---|---|---|---|
| | Total Passes | Non-Routine Passes (e.g. Anomaly Handling/SW Updates) | Failed Passes |
| Weilheim, Germany<br>Neustrelitz, Germany<br>Inuvik, Canada<br>O'Higgins, Antarctica<br>Svalbard, Norway | 424 | 64 | 3 |

**Table 7-2 S-Band Ground Station Passes**

### 7.3.2 X-Band

| X-Band Ground Stations | 01.01.2023 to 31.03.2023 | |
|---|---|---|
| | Executed Passes | Successful Passes |
| Neustrelitz, Germany | 194 | 180 |

**Table 7-3 X-Band Ground Station Passes**

Work is ongoing to integrate Inuvik, Canada, as an additional X-Band ground station in Q2/2023. As a result, more data and more flexibility in X-band data reception are expected, especially concerning image acquisitions over Europe.

## 7.4 Processors

[3] provides the product specification and [4], [5], [6], [7] the algorithm theoretical basis for Level 1B, Level 1C and Level 2A (land / water).

In the reporting period (01.01.2023-31.03.2023) there were two processor updates:

1. **Version 01.02.00 (07.03.2023, available to users on 28.03.2023)**
   This version includes the following changes:
   - Added destriping function for across-track stripes.
   - Fixed a problem in AOCS extraction, resulting in better co-registration accuracy (see Geometric calibration).
   - Implemented interpolation and extrapolation of VNIR radiometric calibration and RNU coefficients, to reduce effects of VNIR degradation.
   - Changed spectral regions for interpolation in L2A to 1331.0 - 1460.0nm and 1796.0 - 1938.0nm.
   - Updated handling of VC AUX data (see also 4.3)
   - Improved determination of L0 product status considering VC AUX sensor parameters by priority and condition.
   - HDR files delivered with BIP, BSQ, BIL products now contain additional information: FWHM, data ignore value, wavelength units
   - Metadata entry ozoneValue is now written for all LX levels, not just L2A.
   - Product status is now reduced if the sun elevation angle is 0 or smaller.
   - Fixed a problem in the calculation of the viewing/incidence angles.

2. **Version 01.02.01 (02.04.2023, available to users on 2)**
   This version includes the following changes:
   - The MIP version written to the log file was corrected.
   - Fixed a crash occurring in L2A jobs whenever Cirrus correction was activated.

The following limitations are applicable as of 31.03.2023:

- The SWIR-A compressor cooler produces a micro-vibration pattern of horizontal stripes on SWIR bands with strong spectral gradients. Still, all spectral and radiometric requirements are within the specification of the mission. An improvement of the processor is planned for mitigating that effect by middle of 2023.
- Defective snow spectrum below 750 nm when snow is confused with clouds by the atmospheric correction processor

The following changes are expected to be performed by 30.06.2023:

- Processor updates after update of SWIR bands configuration for Earth acquisitions
- Fix snow spectra / cloud mask to solve issue with snow spectra
- Correction for SWIR along-track striping
- Correct a defect in the speed of light correction for absolute geometric accuracy of Earth products

## 7.5 Calibrations

The continuous degradation of the VNIR sensor was monitored and quantified. The rate of degradation is constantly decreasing as illustrated in Figure 7-1 and by the end of March 2023 it has reached the point where it is practically negligible.

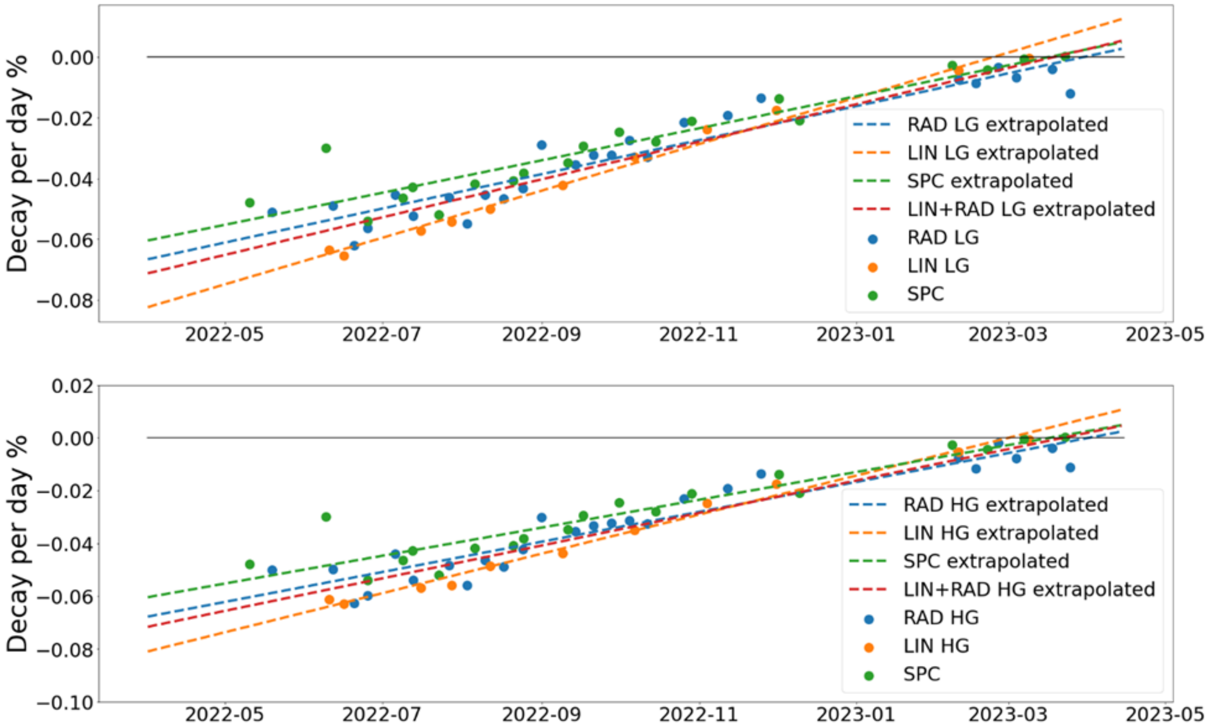


**Figure 7-1 Daily degradation of the VNIR sensor for low gain (top) and high gain (bottom). Estimations based on relative radiometric (RAD), spectral (SPC) and linearity (LIN) calibration measurements for low gain (LG) and high gain (HG). The long-term behavior is linearly extrapolated**

The computed radiometric coefficients are illustrated in Figure 7-2 for five selected spectral bands in VNIR. From one Sun calibration to the next, the coefficients are seen to jump, increasing in value over time. It is most pronounced in the edge bands, see e.g. bands 5 and 85. This effect is reducing over time and by the end of March 2023 is negligible.

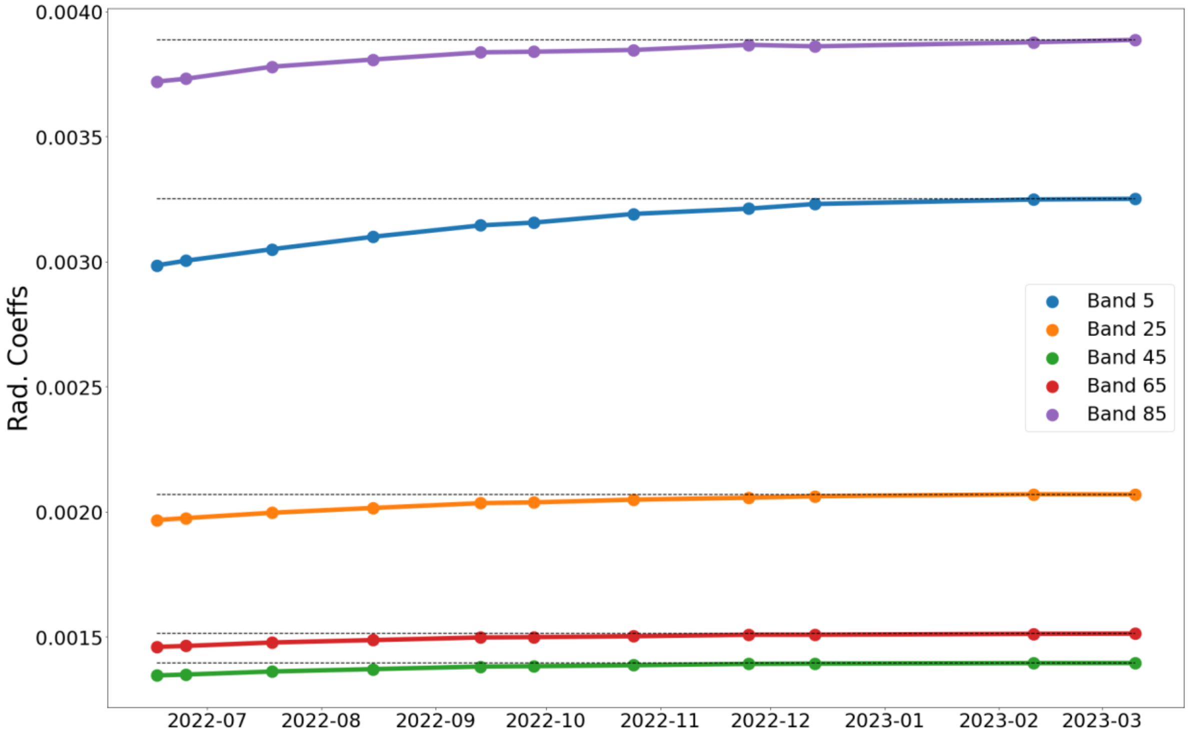


**Figure 7-2 Radiometric coefficients over time for five selected bands. The dashed lines denote the most recent value.**

Figure 7-3 shows the cumulative change in performance as a function of time for VNIR and SWIR sensors, obtained from the linearity calibration measurements.

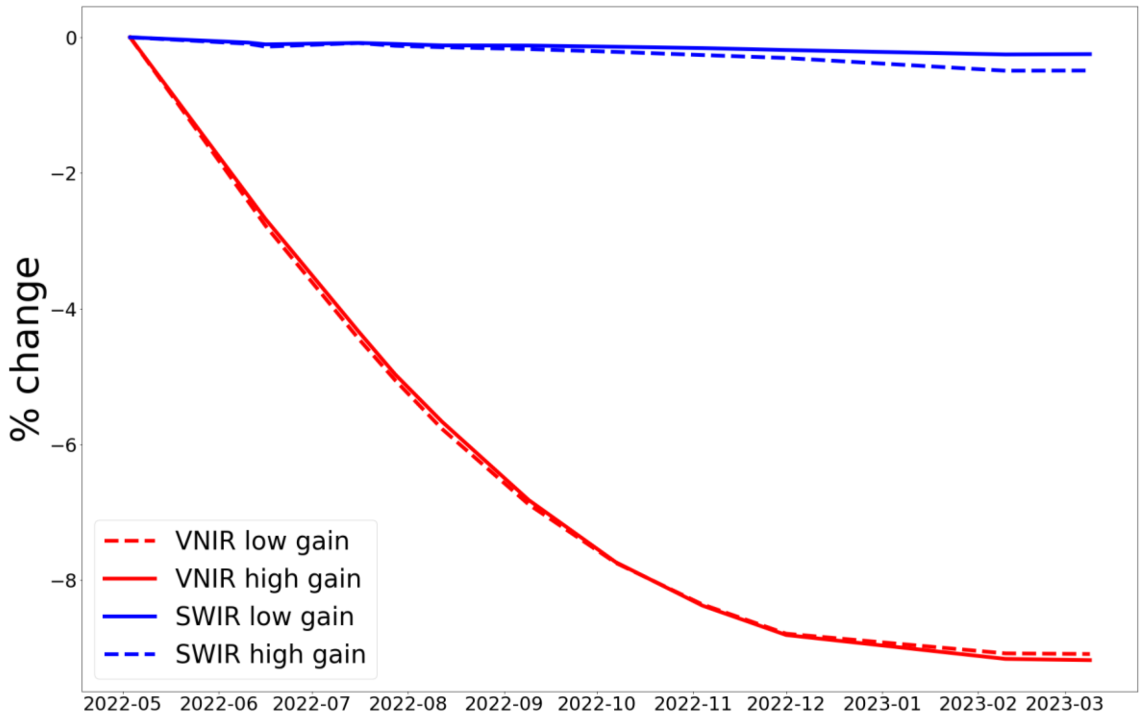


**Figure 7-3 Average percentage change in the linearity reference measurements since launch for VNIR and SWIR in high and low gains**

### 7.5.1 Dead Pixels

The following table shows the number and percentage of dead pixels. Figure 7-4 and Figure 7-5 show the position of the dead pixels in the focal plane of VNIR and SWIR sensors respectively.

| Defect Pixels | 01.01.2023 to 31.03.2023 | |
|---|---|---|
| | Number of Pixels | Percent |
| Total | 1921 | 0.8 |
| VNIR | 137 | 0.2 |
| SWIR | 1784 | 1.2 |

**Table 7-4 Number and percent of dead pixels**

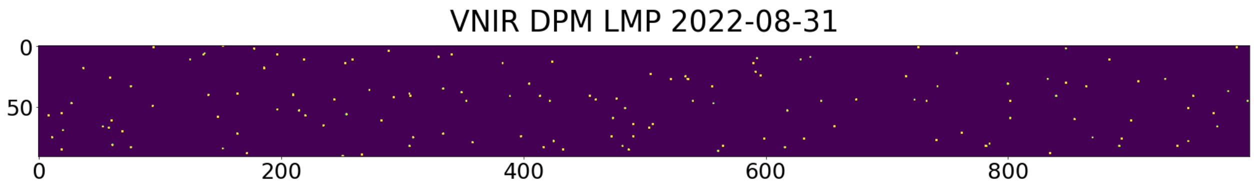


**Figure 7-4 VNIR Dead Pixel Mask**

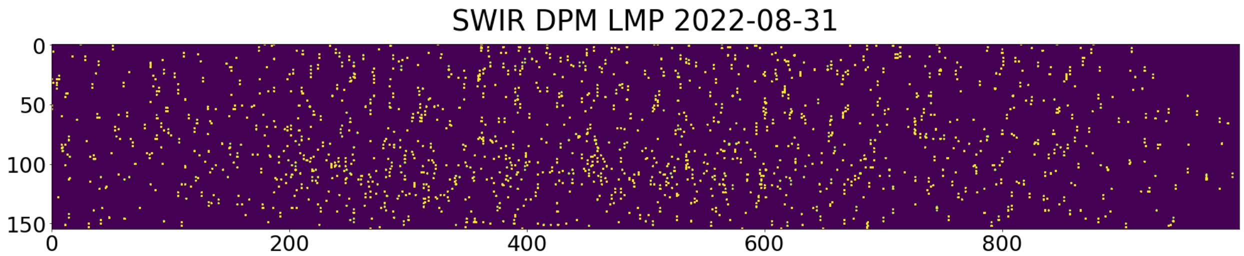


**Figure 7-5 SWIR Dead Pixel Mask**

There are no clusters of more than three spectrally or spatially adjacent dead pixels.

### 7.5.2 Spectral Calibration

Remark: In the following figures, OBCA is abbreviation for On-Board Calibration Assembly for spectral and radiometric calibrations.

| Category | 01.01.2023 to 31.03.2023 | |
|---|---|---|
| | Number of Archived Observations | Size (in GB) |
| Total | 4 | 3.6 |
| Spectral Calibration | 4 | 3.6 |

**Table 7-5 Number and size of archived spectral calibration observations**

The spectral properties – in particular center wavelength (CW) (see Figure 7-6 and Figure 7-7) and full width at half maximum (FWHM) (see Figure 7-8) for each band (spectral coordinate) and pixel (spatial coordinate) – have been characterized, considering all bands and pixels provided in Level 1B, Level 1C and Level 2A products.

The major conclusions of the monitoring of the spectral performance is summarized as follows:

- During the reporting period, 4 spectral calibration measurements were made. These took place on: 07.02.2023, 20.02.2023, 07.03.2023, 22.03.2023.
- The VNIR spectral range in this reporting period was found to be 418.4 – 993.3 nm over 91 bands. The average spectral sampling distance was 6.4 nm with a total range of 4.7 – 8.2 nm. This meets the requirement for overall wavelength coverage [HSI-POSS-0210 [AR-2]], average spectral sampling distance [HSI-POSS-0310] and spectral sampling distance range [HSI-POSS-0320].

- The SWIR spectral range in this reporting period was found to be 902.0 – 2445.3 nm over 155 bands. The average spectral sampling distance was 10.0 nm with a total range of 7.5 – 12.0 nm. This meets the requirement for overall wavelength coverage [HSI-POSS-0210], average spectral sampling distance [HSI-POSS-0310 [AR-2]] and spectral sampling distance range [HSI-POSS-0320].
- The spectral calibration measurements from this quarter show generally good temporal stability – the first measurements after the outage showed a 0.2-03 nm change in VNIR (Figure 6) and a 0.3-0.5 nm change in SWIR, resulting in a spectral calibration update, but the later measurements showed a relatively smaller change in wavelength. All changes were below the 0.69 nm requirement between measurements for VNIR and below the 0.86 nm requirement between measurements for SWIR. This meets the requirement for consecutive spectral stability [HSI-POSS-0510] and overall spectral stability [HSI-POSS-0520].
- FWHM for VNIR and SWIR are shown below but are not recalculated inflight.
- New calibration and reference tables were generated in this reporting period for 7th February 2023.
- The VNIR degradation is visible in the spectral reference calibration measurements acquired in this period, totaling -0.2% across all pixels from 09.12.2022 to 22.03.2023. This is lower than the value of -1.7% reported in the previous quarter.

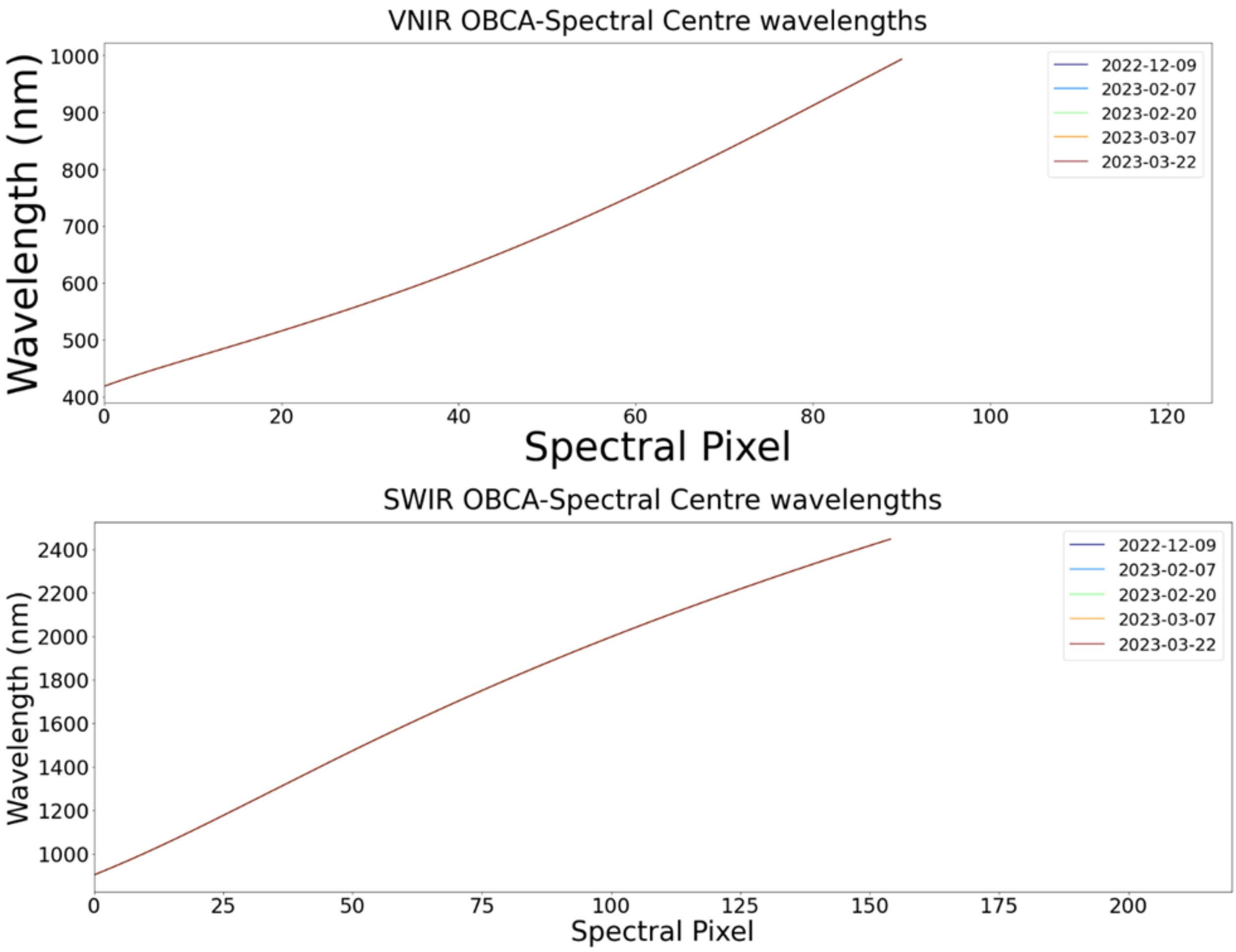


**Figure 7-6 VNIR (top) and SWIR (bottom) center wavelength in nm**

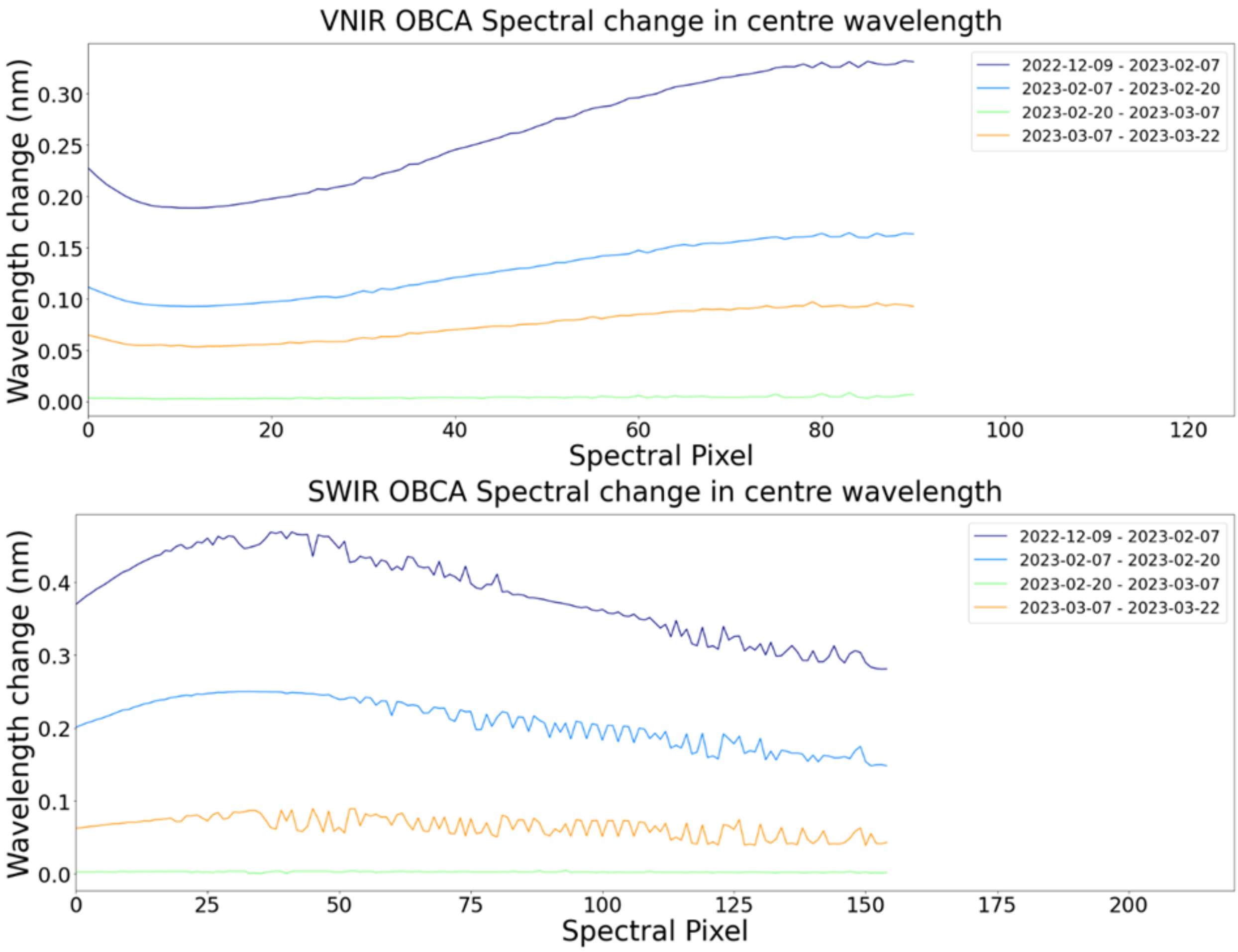


**Figure 7-7 Change in center wavelength per spectral pixel for VNIR (top) and SWIR (bottom)**

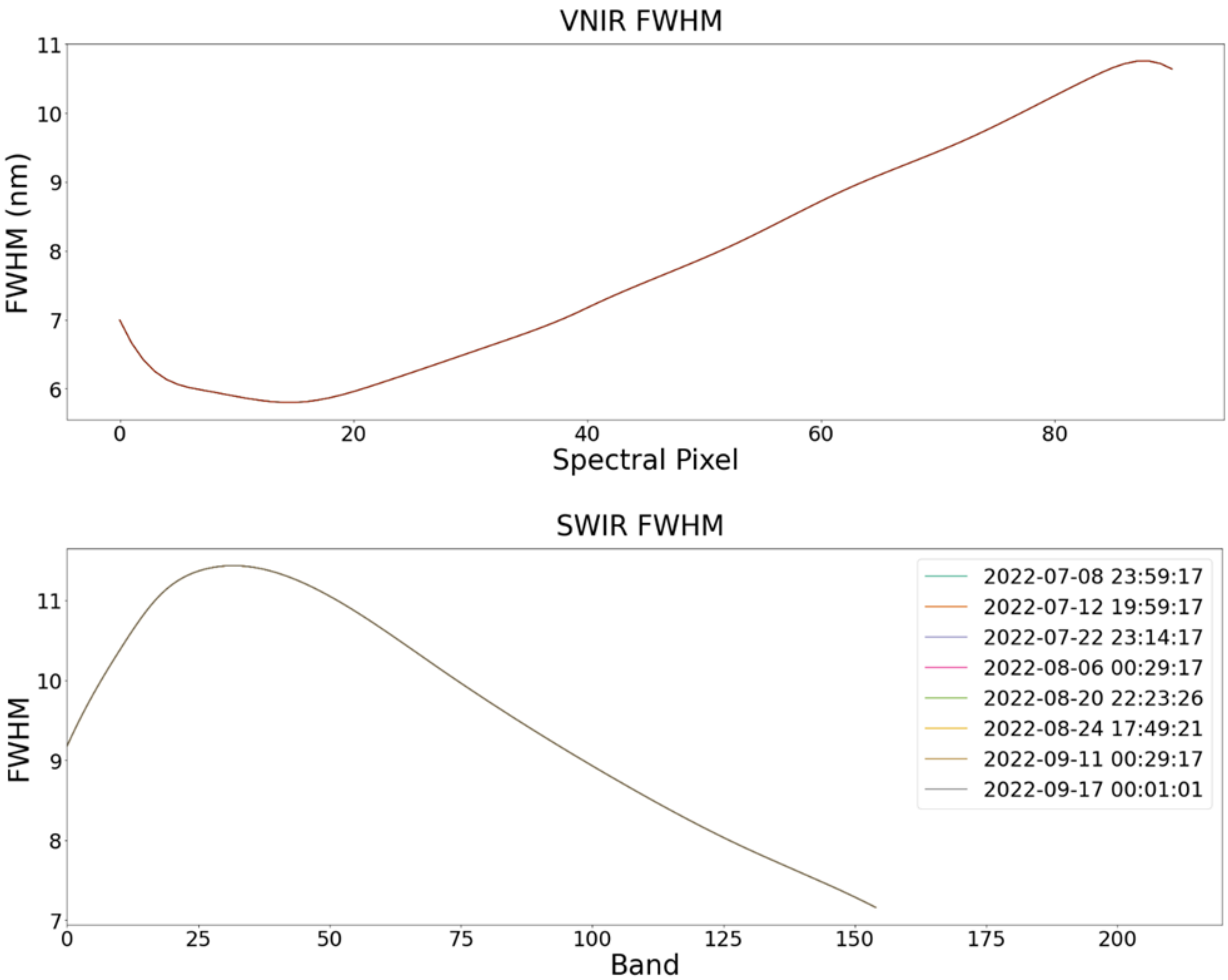


**Figure 7-8 VNIR (top) and SWIR (bottom) FWHM in nm**

CW and FWHM are available in the spectral calibration tables (see Table 7-6) and System Response Functions (SRF) per band are modelled by a Gaussian shape using those parameters.

| Product | Type | Date of Generation | Date of Validity Start | Date of Validity End | Delivered to |
|---|---|---|---|---|---|
| ENMAP01-CTB_SPC-20230208T000000Z_V030000_20230208T155806Z | CTB_SPC | 08.02.2023 | 08.02.2023 | - | DIMS |
| ENMAP01-REF_SPC-20230208T000000Z_V030000_20230208T155806Z | REF_SPC | 08.02.2023 | 08.02.2023 | - | DIMS |

**Table 7-6 Generated spectral calibration tables**

### 7.5.3 Radiometric Calibration

| Category | 01.01.2023 to 31.03.2023 | |
|---|---|---|
| | Number of Archived Observations | Size (in GB) |
| Total | 12 | 62.6 |
| Deep Space | 2 | 2.6 |
| Rel. Radiometric | 6 | 23.4 |
| Abs. Radiometric | 2 | 2.6 |
| Linearity | 2 | 34 |

**Table 7-7 Number and size of archived radiometric calibration observations**

The radiometric properties – characterized in particular by the calibration coefficient for each band (spectral coordinate) and pixel (spatial coordinate) and radiance – during this reporting period are investigated, considering all bands and pixels and radiances provided in Level 1B, Level 1C and Level 2A products.

Both sensors feature two gain settings each. VNIR applies a quantization of 13 bits using a pixel-individual automatic gain switching, where the low gain value is automatically selected, if the signal exceeds a defined threshold. SWIR applies a fixed gain setting, where bands below 1980 nm take the low gain value and bands above 1980 nm take the high gain value.

Radiometric calibration coefficients (see Figure 7-9, Figure 7-10 and Table 7-8) and VNIR RNU (response non-uniformity) (see Figure 7-12) are affected by the degradation of the VNIR sensor and the (expected) change after launch of the SWIR sensor. In-flight, the gain matching coefficients (see Figure 7-11), the SWIR calibration coefficients, and the SWIR RNU (response non-uniformity) (see Figure 7-12) have been stable.

During the reporting period, 2 Absolute Radiometric calibration measurements were obtained. These took place on: 10.02.2023 and 10.03.2023. Owing to the degradation in the VNIR sensor, new calibration and reference tables were created for each new absolute radiometric measurement. Although the VNIR degradation has almost stopped, the overall effects are visible in the reference measurements of the sun. However geometric conditions (sun-earth distance, pointing angle) also play a role in the absolute magnitude so the degradation cannot be quantified with these reference measurements.

The VNIR degradation, although coming to a stop, has directly affected the radiometry. Even though the EnMAP radiometric quality was well within the requirements, the absolute calibration measurements were taken at monthly intervals. As the degradation is now much smaller than last year, and changes between measurements at comparable to the SWIR sensor, calibration acquisitions may be made at longer time intervals in the future.

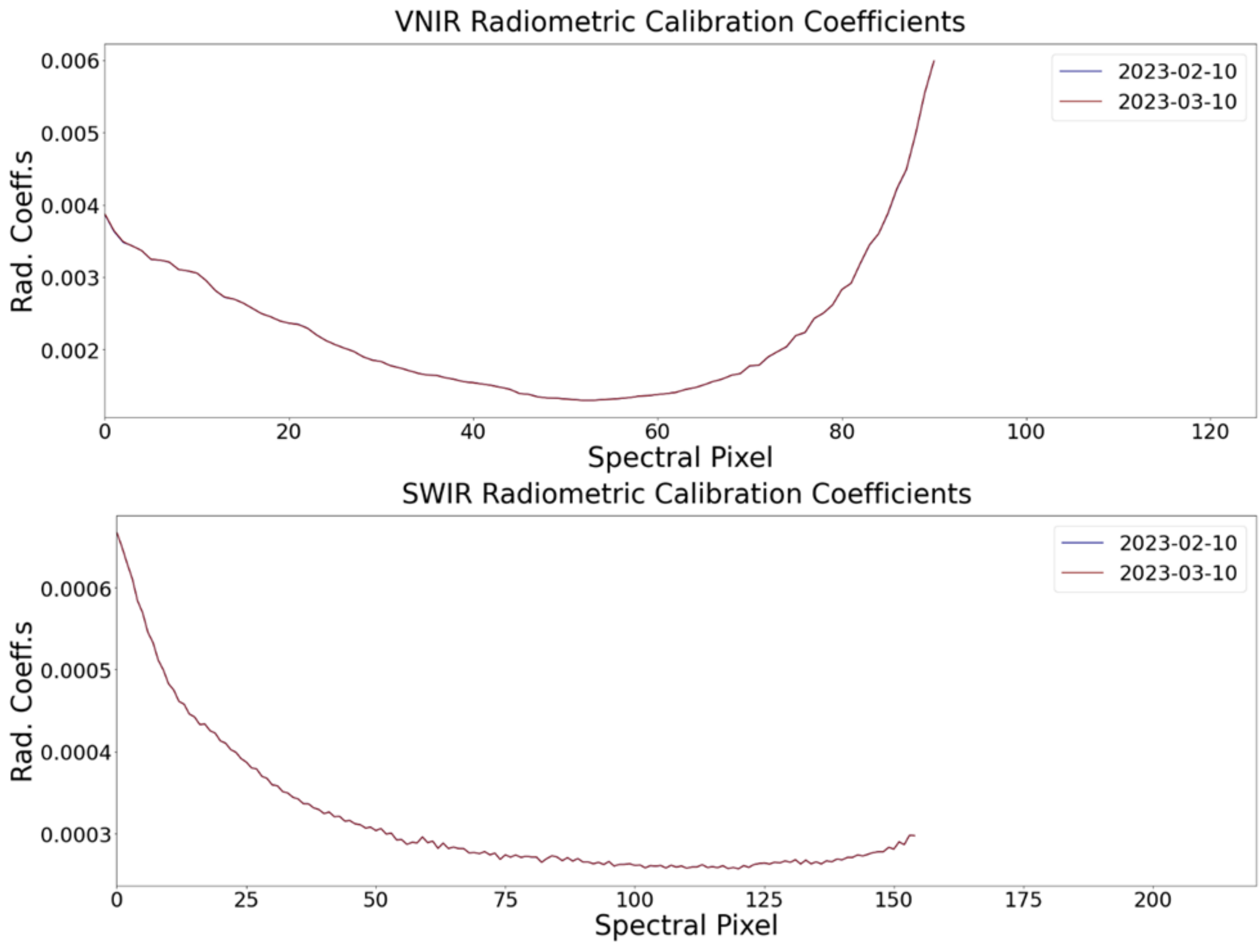


**Figure 7-9** **VNIR (top) and SWIR (bottom) calibration coefficient in mW/cm²/sr/µm**

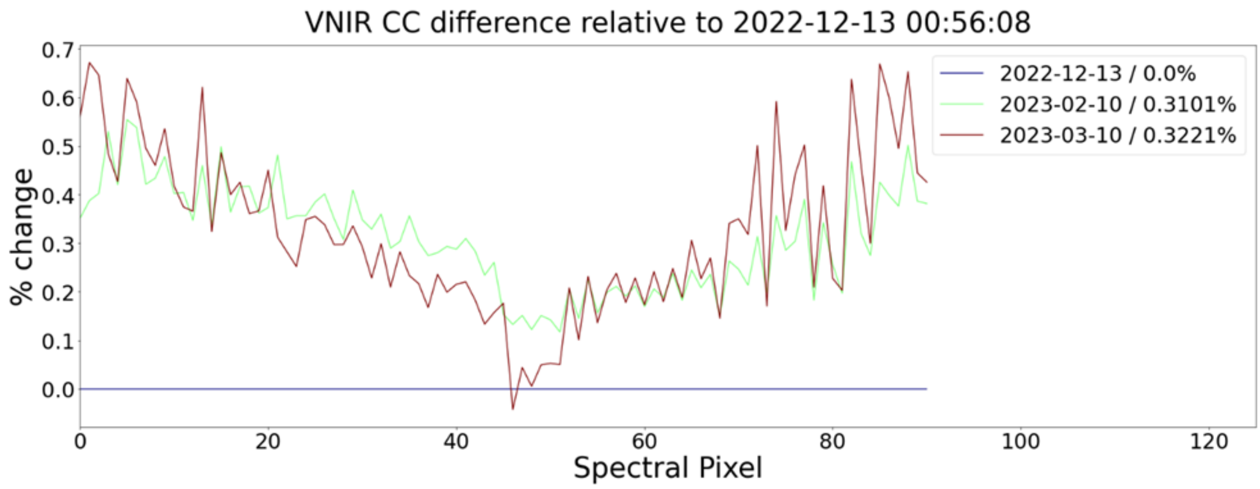

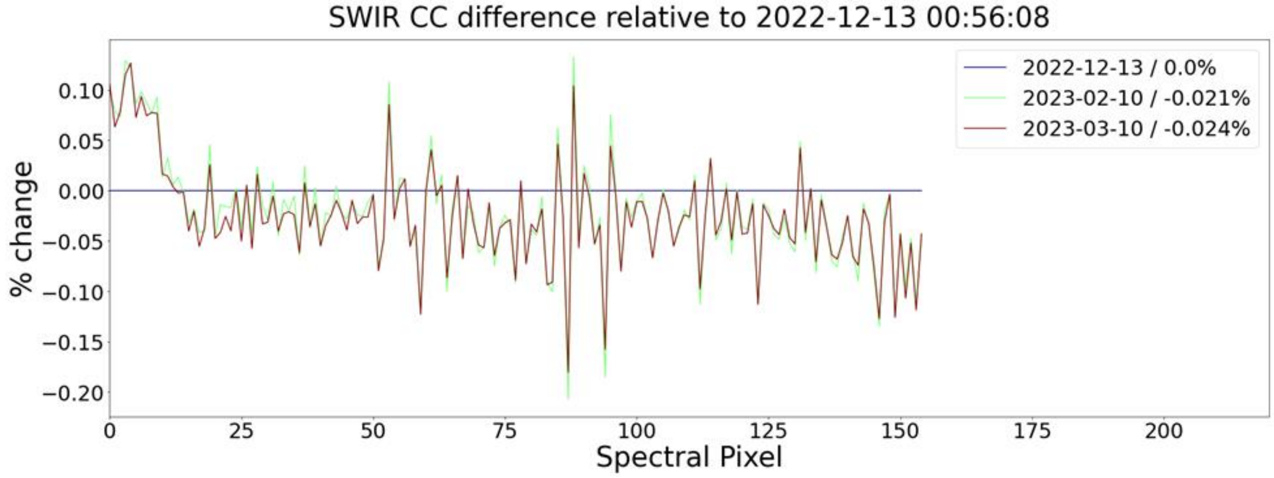


**Figure 7-10 Percentage change in VNIR Calibration Coefficients (top) and SWIR Calibration Coefficients (bottom)**

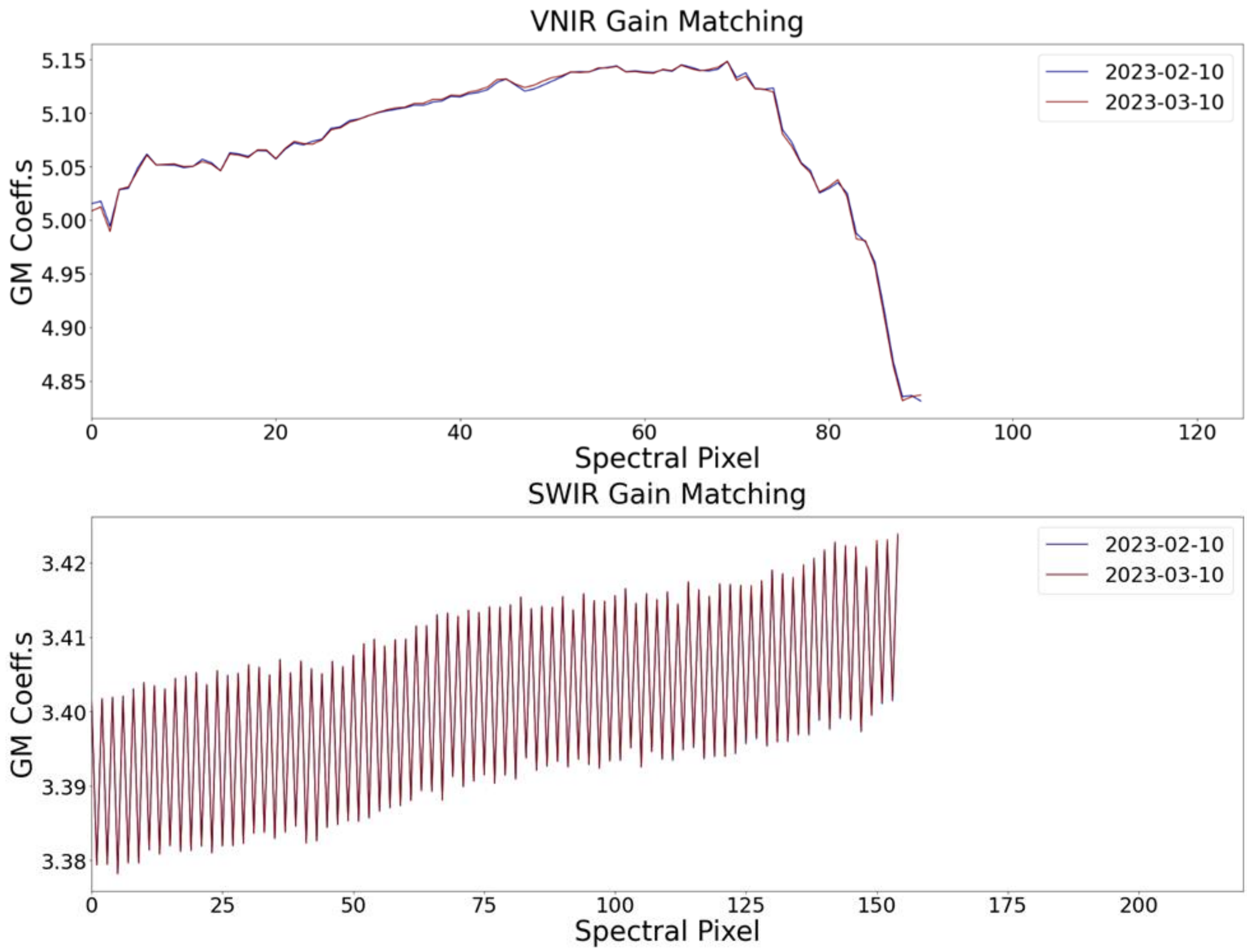


**Figure 7-11 VNIR (top) and SWIR (bottom) gain matching calibration coefficients**

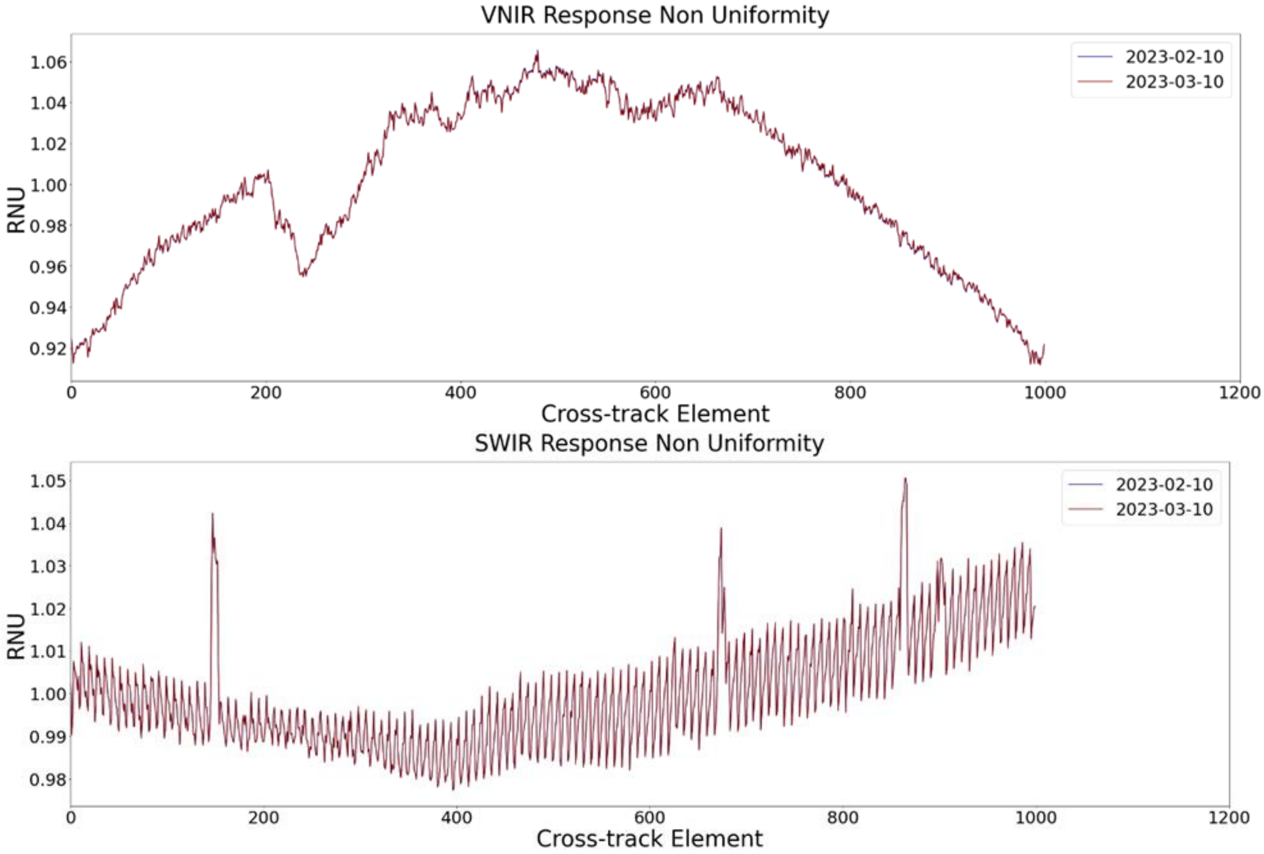


**Figure 7-12 VNIR (top) and SWIR (bottom) response non-uniformity coefficients**

The Signal-to-Noise Ratio (SNR) is derived from the Linearity reference measurements. This is not a perfect set-up for the assessment of the SNR as the linearity measurements only cover a single wavelength and light level at increasing integration times. However, it is well constrained, covering a wide range of radiances including the levels of the solar reference spectrum (30% reflectance, 30° sun incidence angle, 21 km visibility, target 500 m above sea level). The lamp reference measurements are not used, as the reference spectrum is not well covered at the radiances of the lamp and extrapolation would be required to test the performance at the SNR requirements: SNR greater than 500 at 495 nm in VNIR for the solar reference spectrum value; and SNR greater than 150 at 2200 nm in SWIR for the reference spectrum.

For the VNIR sensor, the Signal-to-Noise Ratio has changed during commissioning phase as a result of the ongoing degradation. Nevertheless, the high gain and low gain measurements imply that the SNR in each gain are above the requirement of the reference spectrum at 495 nm. In the case of VNIR low gain, the SNR was found to be 630 for the measurement on 08.03.2023. This value is the practically the same as the one reported in previous quarterly report and indicates how this VNIR degradation is reducing over time.

For the SWIR sensor, both gains are above the requirement at 2200 nm, giving an SNR value of 350 in high gain mode from 30.11.2022. Figure 7-13, Figure 7-14, Figure 7-15 and Figure 7-16 show SNR contour maps for each sensor and gain, based on observed linearity measurements from 08.03.2023, and the solar reference spectrum is plotted to show how the SNR is derived in each case.

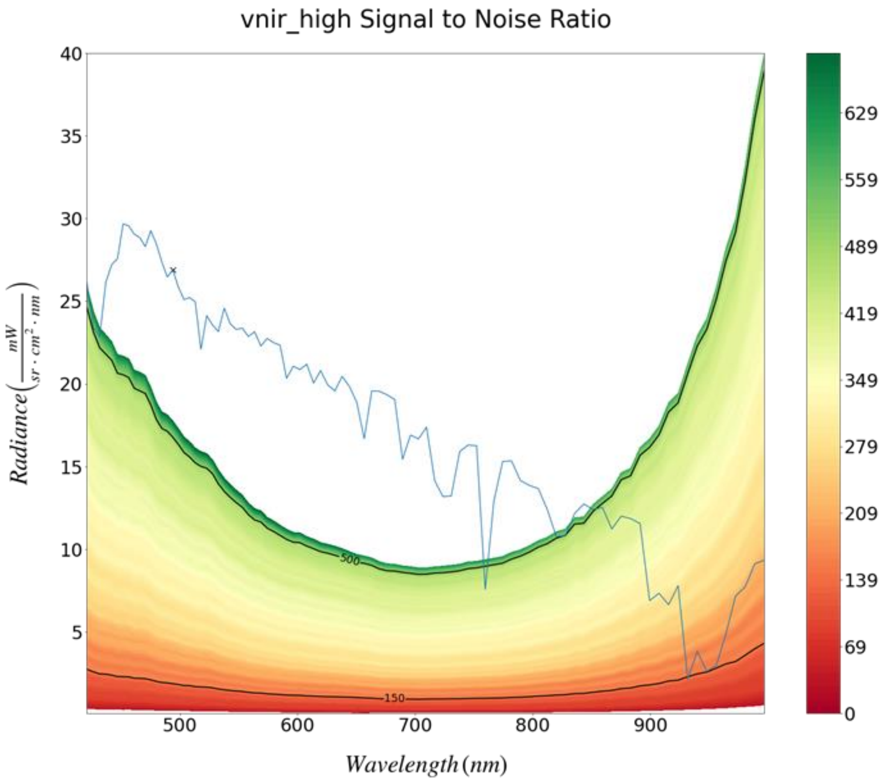


**Figure 7-13** SNR contour map for VNIR high gain from the LED linearity observations observed on 08.03.2023. The solar reference spectrum is shown with a blue line and the position of the requirement is marked on the reference spectrum with a black cross. Contour lines with SNR values of 150 and 500 are also shown in black.

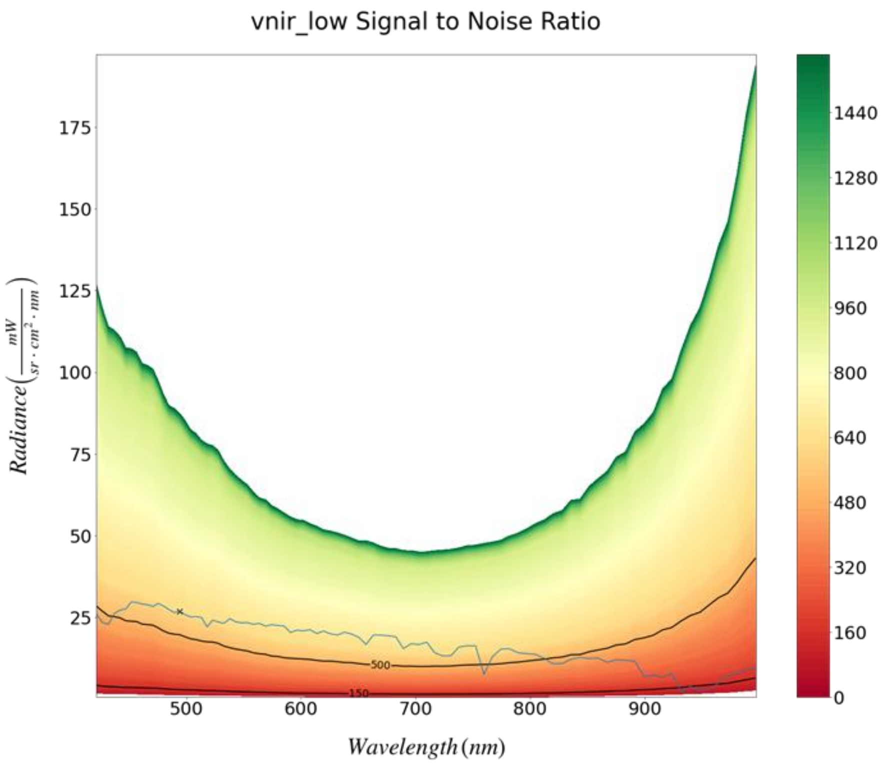


**Figure 7-14** SNR contour map for VNIR low gain from the LED linearity observations observed on 08.03.2023. The solar reference spectrum is shown with a blue line and the position of the requirement is marked on the reference spectrum with a black cross. Contour lines with SNR values of 150 and 500 are also shown in black.

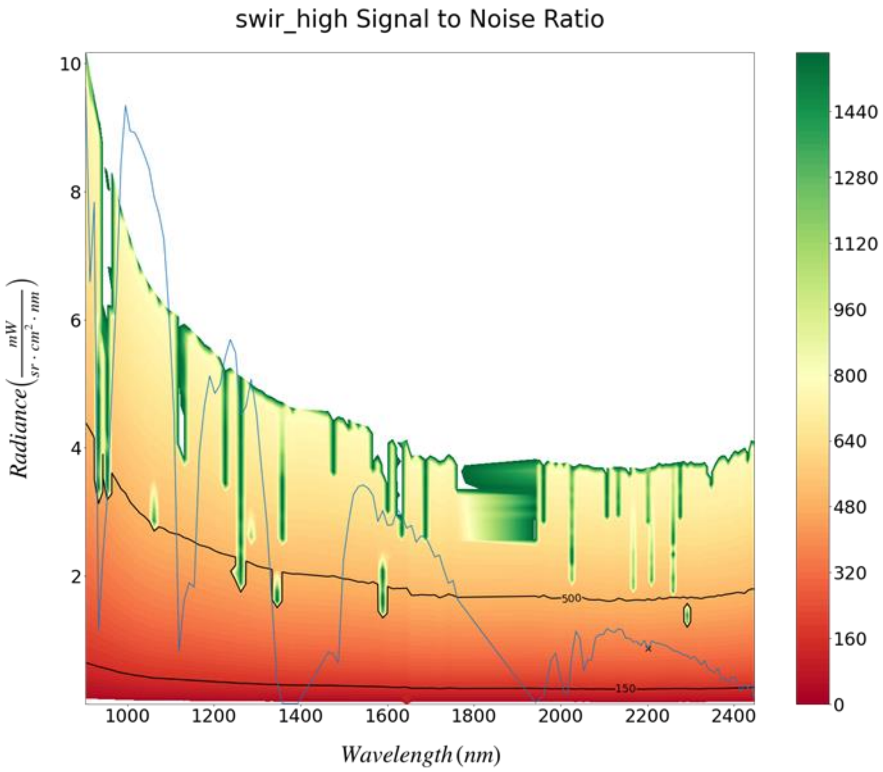


**Figure 7-15** SNR contour map for SWIR high gain from the LED linearity observations observed on 08.03.2023. The solar reference spectrum is shown with a blue line and the position of the requirement is marked on the reference spectrum with a black cross. Contour lines with SNR values of 150 and 500 are also shown in black.

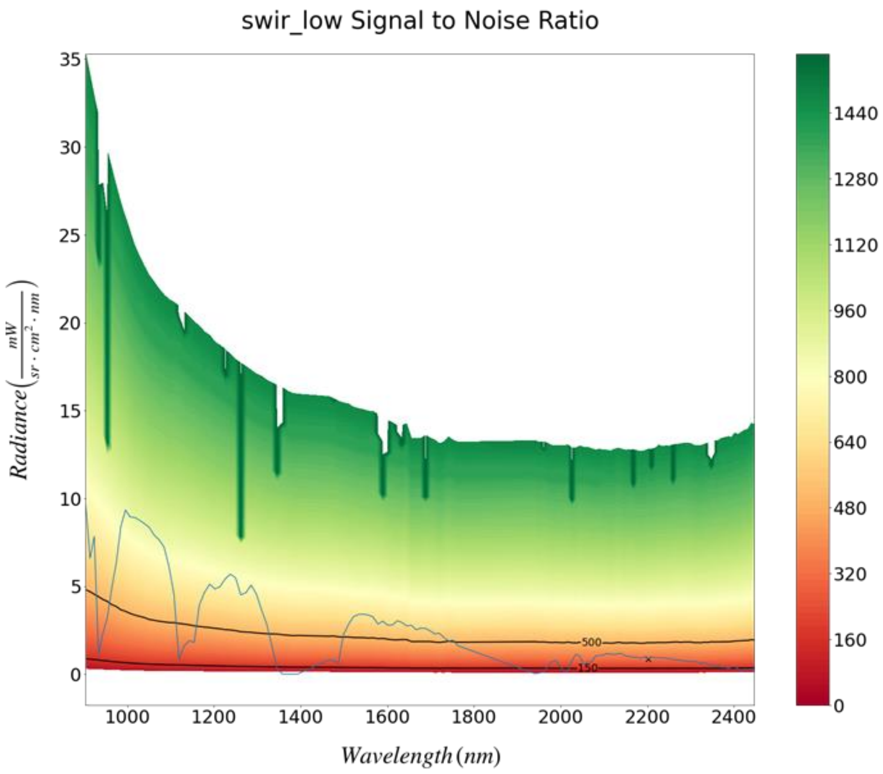


**Figure 7-16** SNR contour map for SWIR low gain from the LED linearity observations observed on 08.03.2023. The solar reference spectrum is shown with a blue line and the position of the requirement is marked on the reference spectrum with a black cross. Contour lines with SNR values of 150 and 500 are also shown in black.

The following calibration products were generated and delivered.

| Product | Type | Date of Generation | Date of Validity Start | Date of Validity End | Delivered to |
|---|---|---|---|---|---|
| ENMAP01-CTB_RAD-20230208T000000Z_V030000_20230217T143611Z | CTB_RAD | 17.02.2023 | Superceded by higher version | Superceded by higher version | DIMS |
| ENMAP01-CTB_RAD-20230311T000000Z_V030000_20230313T082640Z | CTB_RAD | 13.03.2023 | Superceded by higher version | Superceded by higher version | DIMS |
| ENMAP01-CTB_RAD-20220601T000000Z_V040001_20220630T085243Z | CTB_RAD | 27.03.2023 | 01.06.2022 | 17.06.2022 | DIMS |
| ENMAP01-CTB_RAD-20220617T000000Z_V040001_20220630T085243Z | CTB_RAD | 27.03.2023 | 17.06.2022 | 25.06.2022 | DIMS |
| ENMAP01-CTB_RAD-20220625T000000Z_V040001_20220630T092126Z | CTB_RAD | 27.03.2023 | 25.06.2022 | 19.07.2022 | DIMS |
| ENMAP01-CTB_RAD-20220719T000000Z_V040001_20220719T093550Z | CTB_RAD | 27.03.2023 | 19.07.2022 | 15.08.2022 | DIMS |
| ENMAP01-CTB_RAD-20220815T000000Z_V040001_20220817T052543Z | CTB_RAD | 27.03.2023 | 15.08.2022 | 14.09.2022 | DIMS |
| ENMAP01-CTB_RAD-20220914T000000Z_V040001_20220914T131940Z | CTB_RAD | 27.03.2023 | 14.09.2022 | 28.09.2022 | DIMS |
| ENMAP01-CTB_RAD-20220928T000000Z_V040001_20220928T165957Z | CTB_RAD | 27.03.2023 | 28.09.2022 | 25.10.2022 | DIMS |
| ENMAP01-CTB_RAD-20221025T000000Z_V040001_20221025T062338Z | CTB_RAD | 27.03.2023 | 25.10.2022 | 25.11.2022 | DIMS |
| ENMAP01-CTB_RAD-20221125T000000Z_V040001_20230201T090613Z | CTB_RAD | 27.03.2023 | 25.11.2022 | 14.12.2022 | DIMS |
| ENMAP01-CTB_RAD-20221214T000000Z_V040001_20230201T090613Z | CTB_RAD | 27.03.2023 | 14.12.2022 | 08.02.2023 | DIMS |
| ENMAP01-CTB_RAD-20230208T000000Z_V040001_20230217T143611Z | CTB_RAD | 27.03.2023 | 08.02.2023 | 11.03.2023 | DIMS |
| ENMAP01-CTB_RAD-20230311T000000Z_V040001_20230313T082640Z | CTB_RAD | 27.03.2023 | 11.03.2023 | - | DIMS |
| ENMAP01-REF_SUN-20230208T000000Z_V030000_20230217T143611Z | REF_SUN | 17.02.2023 | 08.02.2023 | 11.03.2023 | DIMS |
| ENMAP01-REF_SUN-20230311T000000Z_V030000_20230313T082640Z | REF_SUN | 13.03.2023 | 11.03.2023 | - | DIMS |

**Table 7-8 Generated radiometric calibration tables**

### 7.5.4 Geometric Calibration

A calibration table was created on 10.02.2023 with a validity start date on 11.02.2023. A total of 105 Level 1C products were selected for the calibration. Due to a correction of a software bug in order to improve VNIR-SWIR co-registration accuracy, a new version of this calibration table was created (as well as a new version for the past calibration tables) on 15.02.2023.

As the geolocation accuracy was already well within the requirements (GRD-PCV-0150, GRD-PCV-0155), in this geometric calibration campaign the focus was to improve the co-registration accuracy. In a first try with the same approach as for the last geometric calibration, i.e. matching VNIR and SWIR independently on the reference and determine the respective boresight angles, no improvement could be achieved. Thus, the results of the co-registration QC were used to estimate a correction of the SWIR geometric calibration parameters with respect to the VNIR calibration parameters. This approach improved the co-registration to about 0.2-0.3 pixels, which is in the requirement SRDS-PIM-0050 (including RFW-003 of the space segment). A geometric calibration table was created and used in the processing starting on 11.02.2023 00:00 UTC.

However, there was still room for improvement and after a thorough analysis, a bug could be found in the processor, i.e. the sequence of rotations had to be changed. After this was corrected in the code, the calibration parameters also had to be changed to reflect this change and a new geometric calibration table was generated which can be used in the processing as soon as the processor update (V01.02.00) is installed in Neustrelitz. In first tests the co-registration accuracy improved to 0.05 to 0.15 (mostly below 0.1) pixel.

The re-processing of all data archived before the processor update offers the opportunity to improve also these data wrt. co-registration. Therefore, for each of the existing geometric calibration tables, a new version was created.

| Type of Calibration Table | ID of Calibration Table | Date of Generation | Date of Validity Start | Date of Validity End |
|---|---|---|---|---|
| CTB-GEO | ENMAP01-CTB_GEO-20230211T000000Z_V010100_20230210T135244Z | 2023-02-10 13:52:44 | 2023-02-11 00:00:00.000000 | - |
| CTB-GEO | ENMAP01-CTB_GEO-20230211T000000Z_V010200_20230215T091032Z | 2023-02-15 09:10:32 | 2023-02-11 00:00:00.000000 | - |

**Table 7-9 Generated new geometric calibration tables**

| Datatake/Tile | No. of points | Mean X [pixel] | Mean Y [pixel] | RMSE X [pixel] | RMSE Y [pixel] | Min X [pixel] | Min Y [pixel] | Max X [pixel] | Max Y [pixel] |
|---|---|---|---|---|---|---|---|---|---|
| 10602/001 | 4878 | 0.124 | 0.110 | 0.146 | 0.138 | -0.39 | -0.44 | 0.85 | 1.12 |
| 8418/004 | 7502 | 0.219 | 0.189 | 0.239 | 0.208 | -0.96 | -0.77 | 0.76 | 1.04 |
| 8422/013 | 8809 | 0.136 | 0.109 | 0.149 | 0.131 | -0.60 | -0.51 | 1.13 | 1.96 |
| 8765/009 | 4475 | 0.169 | 0.211 | 0.189 | 0.224 | -0.46 | -0.39 | 0.98 | 0.68 |
| 9303/005 | 7623 | 0.152 | 0.149 | 0.169 | 0.171 | -0.74 | -1.07 | 0.88 | 1.24 |
| 9424/003 | 7290 | 0.131 | 0.164 | 0.145 | 0.179 | -1.19 | -1.51 | 1.04 | 1.21 |
| 9582/033 | 10121 | 0.132 | 0.160 | 0.142 | 0.169 | -0.28 | -0.43 | 0.62 | 0.84 |
| 9593/015 | 7208 | 0.179 | 0.149 | 0.189 | 0.158 | -0.27 | -0.34 | 1.09 | 0.68 |
| 9666/003 | 11841 | 0.054 | 0.163 | 0.086 | 0.172 | -0.45 | -0.32 | 0.59 | 0.74 |
| 9761/002 | 14117 | 0.201 | 0.171 | 0.207 | 0.179 | -0.83 | -1.07 | 0.73 | 1.28 |
| 9761/004 | 13372 | 0.164 | 0.169 | 0.171 | 0.176 | -0.33 | -0.23 | 0.56 | 1.24 |

**Table 7-10 Results VNIR/SWIR co-registration with table ENMAP01-CTB_GEO-20230211T000000Z_V010100_ 20230210T135244Z**

| Datatake/Tile | No. of points | Mean X [pixel] | Mean Y [pixel] | Min X [pixel] | Min Y [pixel] | Max X [pixel] | Max Y [pixel] | RMSE X [pixel] | RMSE Y [pixel] |
|---|---|---|---|---|---|---|---|---|---|
| 1498/001 | 6241 | -0.060 | 0.088 | -31.09 | -0.2 | 1.12 | 14.98 | 0.407 | 0.216 |
| 1498/002 | 5939 | -0.024 | 0.110 | -0.93 | -0.99 | 1.06 | 0.54 | 0.085 | 0.125 |
| 1498/003 | 5162 | -0.132 | 0.059 | -0.39 | -0.25 | 0.52 | 0.44 | 0.152 | 0.771 |
| 3738/001 | 1954 | 0.109 | 0.011 | -0.22 | -0.35 | 0.58 | 1.08 | 0.126 | 0.064 |
| 3738/002 | 2335 | 0.084 | -0.079 | -0.23 | -0.43 | 0.57 | 0.35 | 0.110 | 0.128 |
| 3738/003 | 3116 | 0.078 | -0.135 | -0.23 | -0.55 | 0.51 | 0.46 | 0.105 | 0.172 |
| 4321/001 | 4853 | 0.157 | 0.098 | -0.15 | -0.33 | 1.06 | 0.56 | 0.169 | 0.109 |
| 4321/002 | 3856 | 0.042 | 0.085 | -0.21 | -0.23 | 0.43 | 0.44 | 0.069 | 0.098 |

**Table 7-11 Results VNIR/SWIR co-registration with table ENMAP01-CTB_GEO-20230211T000000Z_V010200_ 20230215T091032Z and after fixing the software**

## 7.6 Internal Quality Control

### 7.6.1 Archive

Within the given time period (01.01.2023 – 31.03.2023), 661 datatakes with a total of 5183 tiles were acquired and archived (remark: additional datatakes acquired during this period but for which the archiving is pending might be missing in the statistics).

The overall quality rating statistics are listed in Table 7-12, and in relation to the Solar Zenith Angle (SZA) in Table 7-13. Also these ratings are further detailed for the VNIR and SWIR detector in Table 7-14, showing a nominal performance rating for the given quality thresholds.

In addition, the rating for the atmospheric conditions for the scenes are depicted in Table 7-15When setting the atmospheric quality rating in relation to the illumination conditions (i.e., large SZA) during data acquisition (Table 7-16), 49% of the “reduced quality” ratings and over 18% of the “low quality” ratings can be related to low Sun angles / night time acquisitions.

In addition, the “low qualityAtmosphere” rating can be further related to high cloud cover (66% of the low qualityAtmosphere tiles) and the unavailability of enough DDV pixels (54%) (see Table 7-16). Consequently, the rating is absolutely reasonable and can be explained.

| Parameter | Value | Percentage | Number of tiles |
|---|---|---|---|
| overallQuality | Nominal | 93% | 4822 |
| | Reduced | 1% | 3 |
| | Low | 7% | 358 |

**Table 7-12 Overall quality rating statistics**

| Parameter | Number of tiles | Sub-Parameter | Number of tiles |
|---|---|---|---|
| overallQuality = Low | 358 | | |
| | | Thereof with SZA > 70° | 358 |

**Table 7-13 Overall quality rating in relation to Sun Zenith Angle (SZA)**

| Parameter | Number of tiles | Sub-Parameter | Number of tiles |
|---|---|---|---|
| overallQuality = Reduced | 3 | | |
| | | Thereof with qualityVNIR nominal | 0 |
| | | Thereof with qualitySWIR nominal | 3 |
| overallQuality = Low | 358 | | |
| | | Thereof with qualityVNIR nominal or reduced | 0 |
| | | Thereof with qualitySWIR nominal or reduced | 358 |

**Table 7-14 Reduced and low quality rating statistics**

| Parameter | Value | Percentage |
|---|---|---|
| QualityAtmosphere | Nominal | 27% |
| | Reduced | 14% |
| | Low | 59% |

**Table 7-15 QualityAtmosphere rating statistics**

| Parameter | Number of tiles | Sub-Parameter | Number of tiles |
|---|---|---|---|
| overallAtmosphere = Reduced | 739 | | |
| | | Thereof with SZA > 60° | 363 |
| | | Thereof with SZA > 70° | 346 |
| | | Thereof with SZA > 80° | 341 |
| overallAtmosphere = Low | 3058 | | |
| | | Thereof with SZA > 60° | 554 |
| | | Thereof with SZA > 70° | 164 |
| | | Thereof with SZA > 80° | 33 |

**Table 7-16 QualityAtmosphere rating in realtion to Sun Zenith Angle (SZA)**

| Parameter | Number of tiles | Sub-Parameter | Number of tiles |
|---|---|---|---|
| overallAtmosphere = Low | 3058 | | |
| | | Thereof with Cloud Cover > 66% | 2081 |
| | | Thereof with DDV warnings | 1655 |

**Table 7-17 QualityAtmosphere rating in relation to Cloud Cover and DDV availability**

### 7.6.2 Level 1B

#### 7.6.2.1 Radiometric Performance

**Indications for defective / de-calibrated detector elements**

Using the Detector Map components, an offline check of possibly defective or de-calibrated detector elements is conducted. In particular, if a detector element is identified as “possibly defective” in at least 75% of the useful tiles. Within the given reporting period, the following indications for defective pixels are found for the VNIR and the SWIR camera:

VNIR (total of 3231 tiles, with 2989 suitable for analysis)

| Band | Cross-track element |
|---|---|
| 19 | 187 |
| 77 | 600 |
| 85 | 14 |
| 89 | 395 |

SWIR (total of 3231 tiles, with 2973 suitable for analysis)

| Band | Cross-track element | Band | Cross-track element |
|---|---|---|---|
| 2 | 235, 286, 593, 673 | 49 | 311, 344, 395 |
| 4 | 362, 363, 418 | 50 | 154, 155 |
| 5 | 687 | 52 | 97, 98 |
| 7 | 910 | 53 | 602, 941 |
| 8 | 801 | 55 | 221, 965 |
| 11 | 715 | 57 | 632, 922 |
| 14 | 29, 684 | 58 | 89, 90 |
| 16 | 535 | 60 | 312 |
| 19 | 84 | 62 | 123 |
| 20 | 84 | 65 | 93 |
| 28 | 104 | 71 | 801, 844, 845 |
| 29 | 855, 928 | 85 | 525 |
| 30 | 360 | 89 | 285 |
| 31 | 360 | 91 | 973 |
| 33 | 560 | 92 | 677, 973 |
| 38 | 241 | 96 | 341, 819 |

| | | | |
|---|---|---|---|
| 47 | 511 | 101 | 318 |
| 48 | 218 | 102 | 925 |
| | | 106 | 107 |
| | | 107 | 265, 764 |
| | | 108 | 886 |
| | | 111 | 315 |
| | | 118 | 837 |

**Indications for increasing dead detector elements**

Within the given reporting period, the statistics for dead pixels are provided in the following tables. When comparing these numbers to the estimates in the EN-GS-RPT-1702 Radiometric Calibration Report, one must bear in mind that the latter is based on the full detector readout configuration, while the numbers provided in the following are related to the standard readout configuration as provided in the user product. Because of the smaller readout area, these following dead pixel numbers are lower in comparison.

| Parameter | Value (number of pix) | Percentage of tiles |
|---|---|---|
| DeadPixelsVNIR | 137 | 100% |

**Table 7-18 Dead pixel statistics, VNIR**

| Parameter | Value (number of pix) | Percentage of tiles |
|---|---|---|
| DeadPixelsVNIR | 1531 | 100% |

**Table 7-19 Dead pixel statistics, SWIR**

**Saturation and radiance levels outside nominal range**

Within the given reporting period, no indications for increased saturation defects are found for the VNIR and the SWIR camera (see Table 7-20 and Table 7-21).

| Parameter | Value (per mille of scene) | Percentage of tiles |
|---|---|---|
| SaturationCrosstalkVNIR | 0 | 91% |
| | > 0 per mille | 9% |
| | > 10 per mille | 1.5% |

**Table 7-20 Saturation statistics, VNIR**

| Parameter | Value (per mille of scene) | Percentage of tiles |
|---|---|---|
| SaturationCrosstalkSWIR | 0 | 96% |

| | | |
|---|---|---|
| | > 0 per mille | 4% |
| | > 10 per mille | <<1% |

**Table 7-21 Saturation statistics, SWIR**

**Other radiometric artifacts**

Within the given reporting period, the striping performance is similar to the one encountered during the Commissioning Phase. Within PCV, different de-striping approaches were tested, and the selected one by M. Brell (GFZ) is implemented in processor version V010200 (07.03.2023).

Apart from this, no indications for an increase in general radiometric artifacts are found for the VNIR and the SWIR camera (see following tables).

| Parameter | Value (number of pix) | Percentage of tiles |
|---|---|---|
| generalArtifactsVNIR | 0 | 0% |
| | > 0 | 100% |
| | > 10 | 11% |
| | > 100 | 7% |
| | > 1000 | 0% |

**Table 7-22 Artifacts statistics (without striping), VNIR**

| Parameter | Value (number of pix) | Percentage of tiles |
|---|---|---|
| generalArtifactsSWIR | 0 | 0% |
| | > 10 | 100% |
| | > 25 | 15% |
| | > 100 | 7% |
| | > 1000 | 0% |

**Table 7-23 Artifact statistics (without striping), SWIR**

#### 7.6.2.2 Spectral Performance

For the analysis of the spectral stability, the Detector Maps of all Earth datatakes acquired in the reporting period were used. Note that no smile correction was applied, so the analysis shows only on the instrument characteristics. At the wavelengths of stable atmospheric features (760 nm Oxygen absorption and CO2 absorption at ~2050 nm), simulations of spectral shifts were carried out by resampling the absorption in the interval of +/- 3.0 nm with steps of 0.05 nm. Then the signal of the Detector Maps and the simulated shifted absorptions were normalized, and a least-square fit was used where the sensed absorption matches the simulations. Also an additional polynomial fitting was applied, as especially the CO2 absorption band region has low signal an is thus significantly influenced by noise.

When repeating this analysis for many Detector Maps, then the spectral behavior over time can be addressed (see Figure 7-17 and Figure 7-18). More important is the standard deviation of the shift, as this represents the spectral stability within the given period. As shown Figure 7-17 and Figure 7-18, the standard deviation (1σ) at 760 nm is better than 0.25 nm for all cross-track elements, and better than 0.65 nm at 2060 nm. Also the cross-track shape shows little variation; in case of the VNIR, the stability is equally good for all cross-track elements, while for the SWIR the shape is similar to the detected center wavelengths deviation.

In summary, these findings agree well with the instrument performance estimated during the Commissioning Phase and Q4 2022.

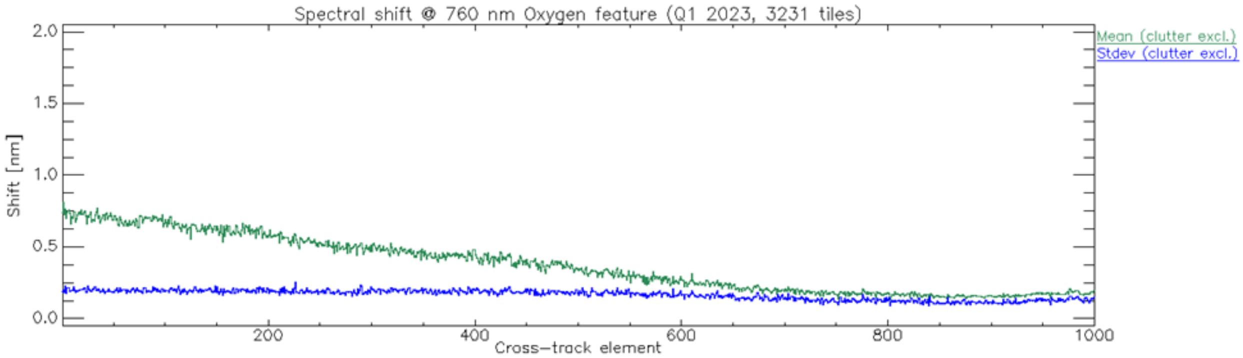


**Figure 7-17 VNIR estimated spectral shift of the bands at 760 nm w.r.t. the nominal band center (same baseline as in CP)**

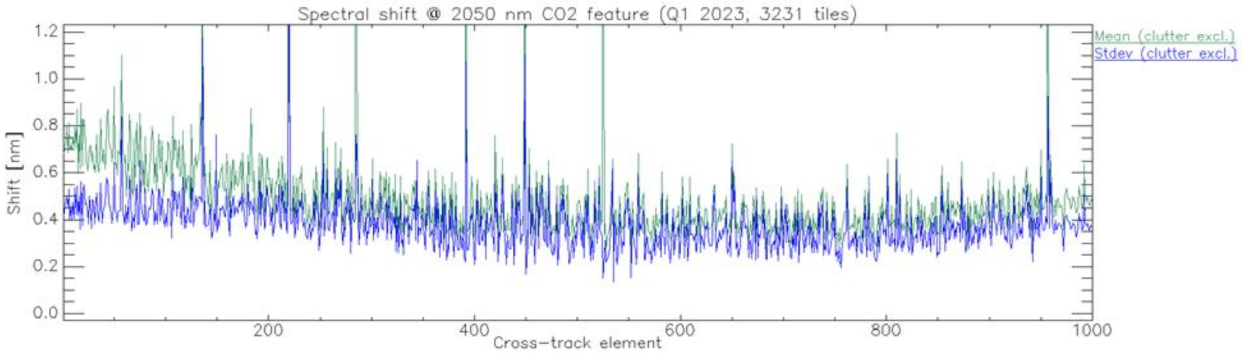


**Figure 7-18 SWIR estimated spectral shift of the bands at 760 nm w.r.t. the nominal band center (same baseline as in CP)**

### 7.6.2.3 Image artifacts

Apart from the three known radiometric artefacts, no indications for an increase in general radiometric/spectral problems are found for the VNIR and the SWIR cameras. The known artefacts are indicated below. In addition, it has been studied the validity of the destriping algorithm included in processor version 01.02.00.

### 1. Validity of across-track de-striping correction after processor update

For the development and the final selection of a destriping algorithms, multiple tests have been conducted by VAL @ GFZ, DEV and QC. In the following, the results of the finally implemented destriping processor (EnMAP processor version 01.02.00 (07.03.2023) and later) for a critical scene (ENMAP01-_____L0-DT0000009666_20230310T015524Z_033, see Figure 7-19) with deep ocean and bright dryland is depicted, nicely illustrating the typical performance.

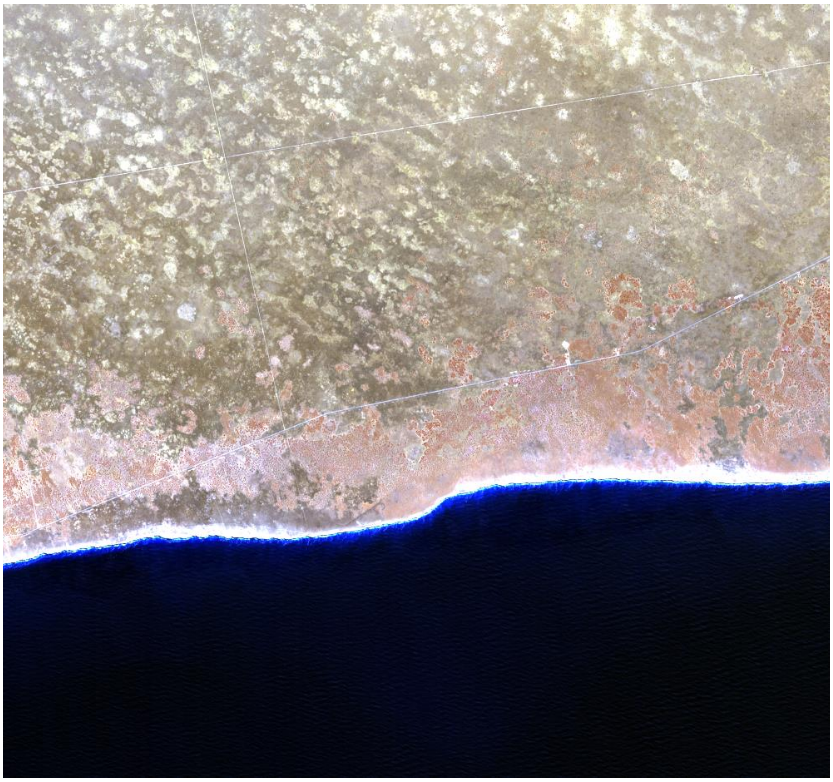

**Figure 7-19 CIR composite for the scene DT9666 (2% linear stretch)**

In the following, examples for top-of-atmosphere radiance products in sensor geometry are given, as the interpolation step in the geocoding affects the image statistics and visual impression. Additionally, the shown internal L1Bint products represent the processing before the striping correction (i.e., fully radiometrically corrected and dead pixels are already interpolated), and the L1Bdestriped are the products after destriping.

For VNIR, the changes in image statistics are small, with ~0.2% for most bands, and up to ~2% around band 80 which is affected by water vapor.

For SWIR, the relative changes are also small for most bands (~0.05% in the low gain region and 0.5% in the high gain region), with the exceptions of larger changes in the atmospheric absorption regions where the signal is small.

As a conclusion, for this and other scenes the image statistics are kept intact by the scene-based statistical destriping.

Next, the bands with the largest differences -and thus the highest striping- are shown in Figure 7-22 and Figure 7-23, for a bright land area in the VNIR. As the performance of the destriping might be different over bright and over dark targets, it is required to assess high radiance as well as low radiance conditions, as illustrated in Figure 7-25 and Figure 7-26 for an area of open ocean in the VNIR. For SWIR, similar figures are shown in Figure 7-28 and Figure 7-29 for a land area. The difference images are depicted in Figure 7-24, Figure 7-27 and Figure 7-32. In order to highlight the effect of the striping, all images are stretched non-linear.

In the given figures and other scenes, the visual image impression is improved, as the striping artefacts are mostly removed. Still some small striping can be seen in the destriped images, but this is mostly due to the extreme image stretch. Also note that the difference images only contain vertical stripes, and no structures from the images are included – this is a good indication that only the striping is corrected, and image content is left intact

In conclusion, the destriping algorithm is valid for low and for high radiance areas, improving the visible image quality while keeping the impact in the image radiometry and thus image statistics small.

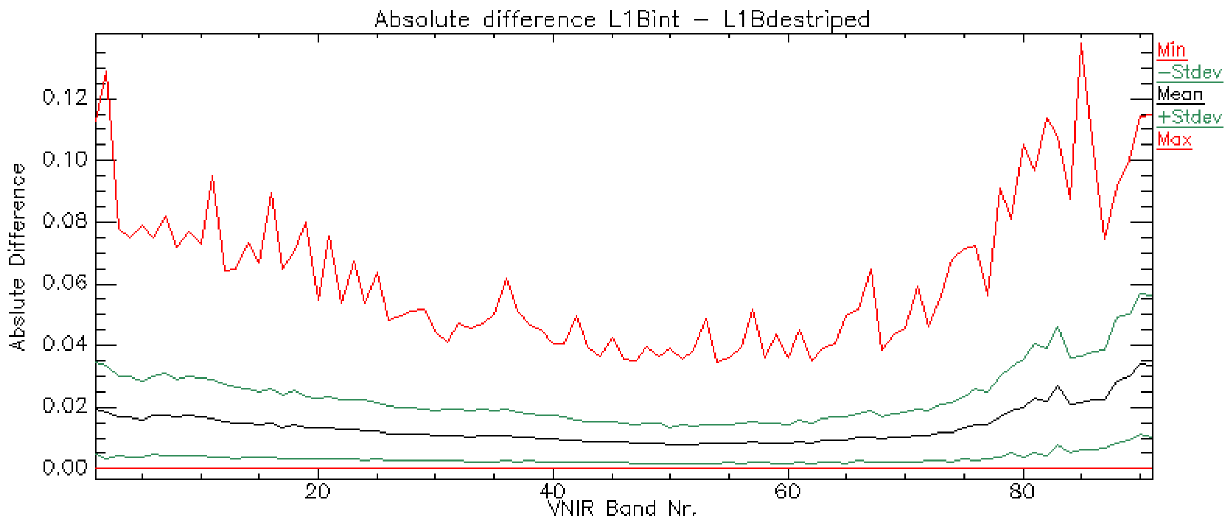


**Figure 7-20 VNIR image statistics of the absolute difference between L1Bint and L1Bdestriped**

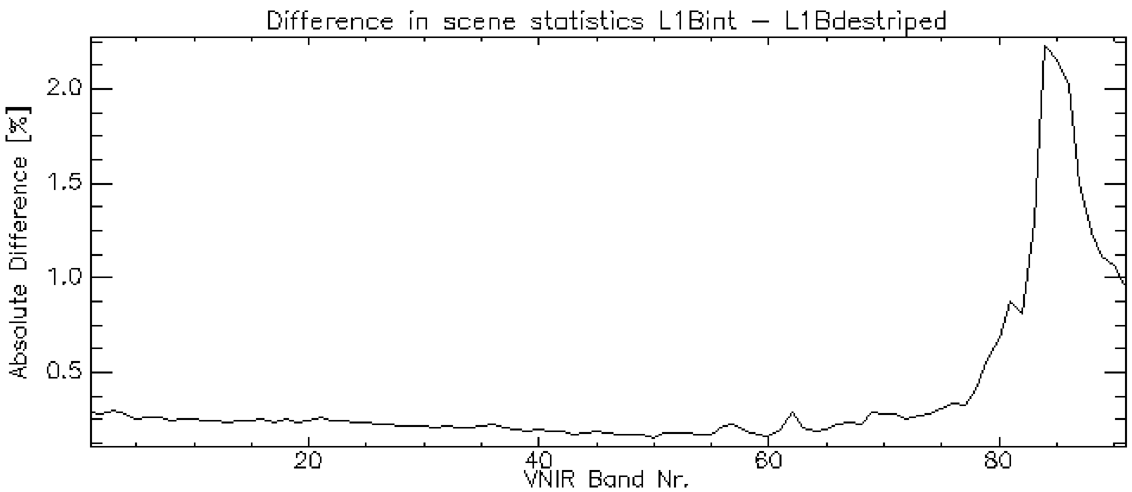


**Figure 7-21 VNIR image statistics of the relative difference between L1Bint and L1Bdestriped**

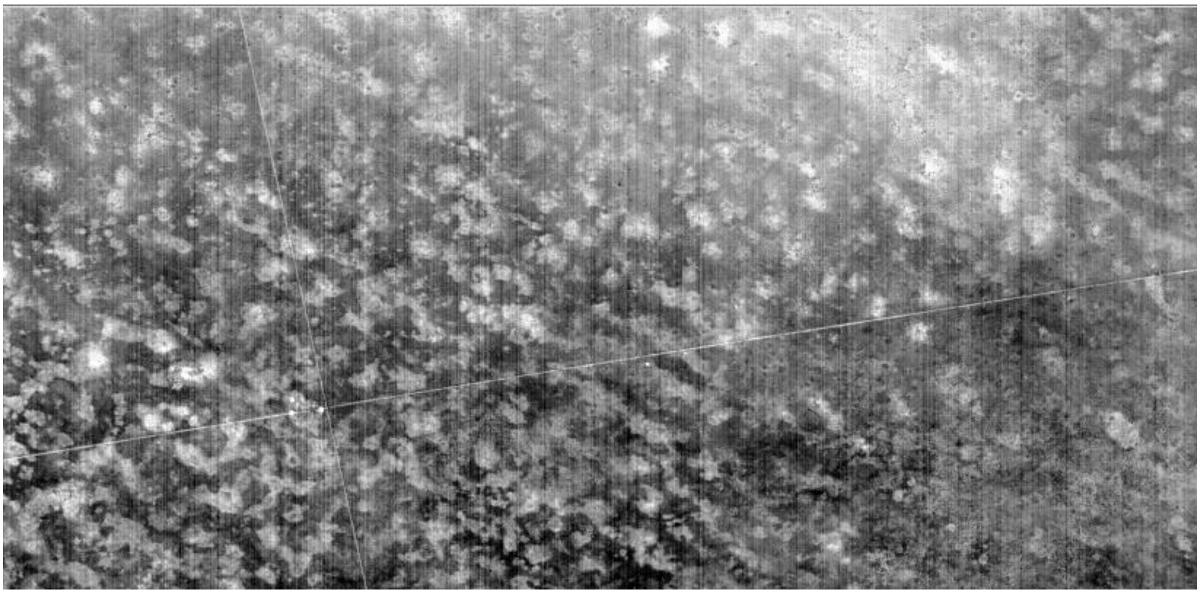

**Figure 7-22 VNIR band 84 over land, L1Bint, non-lin. stretch**

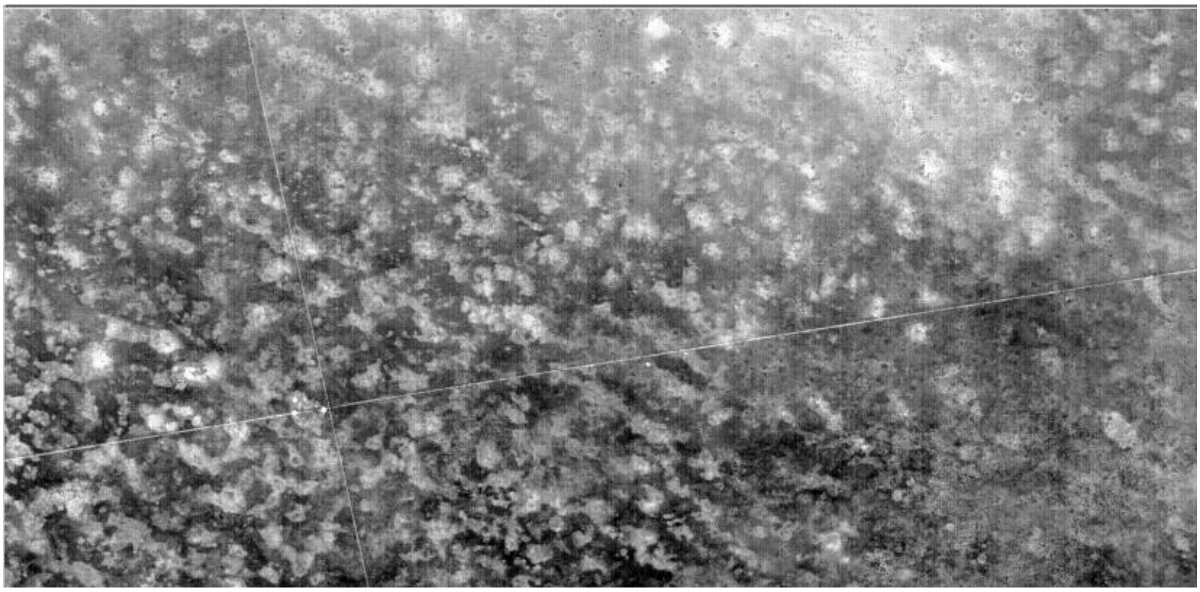

**Figure 7-23 VNIR band 84 over land, L1Bdestriped, non-lin. stretch**

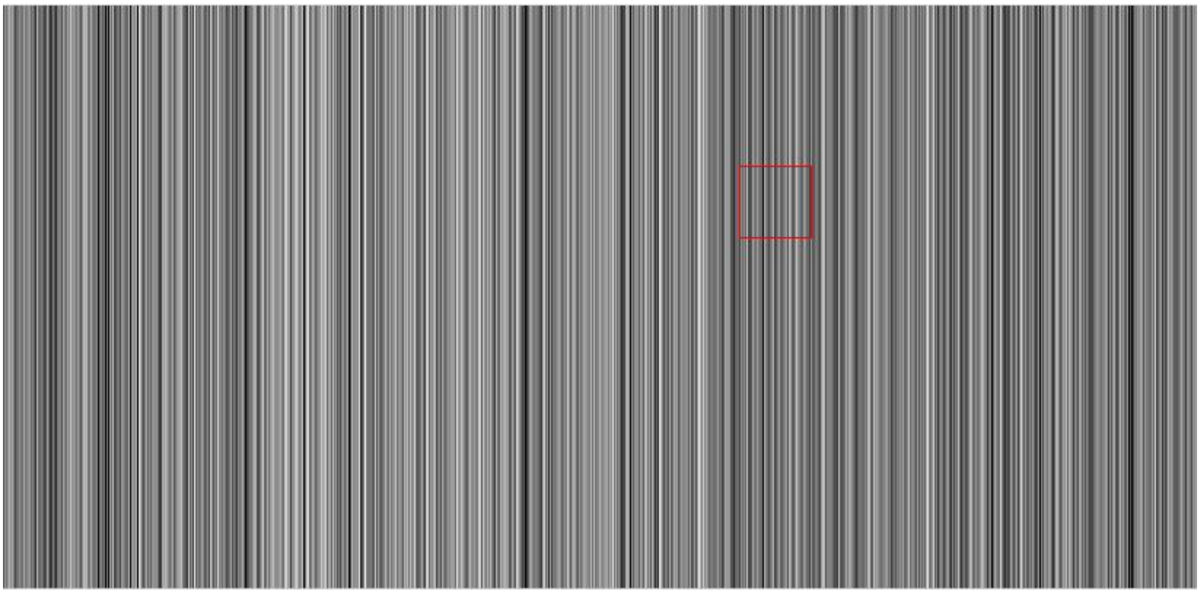

**Figure 7-24 VNIR band 84 over land, abs. difference of L1Bint and L1Bdestribed, non-lin. Stretch**

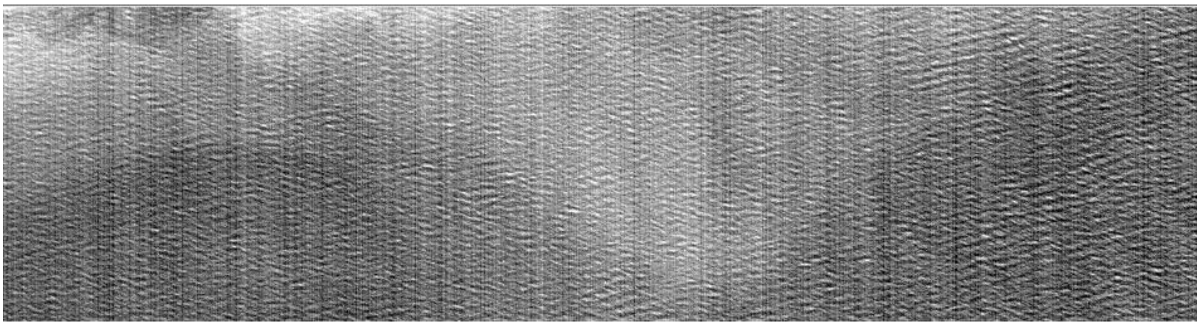

**Figure 7-25 VNIR band 7 over water, L1Bint, non-lin. stretch**

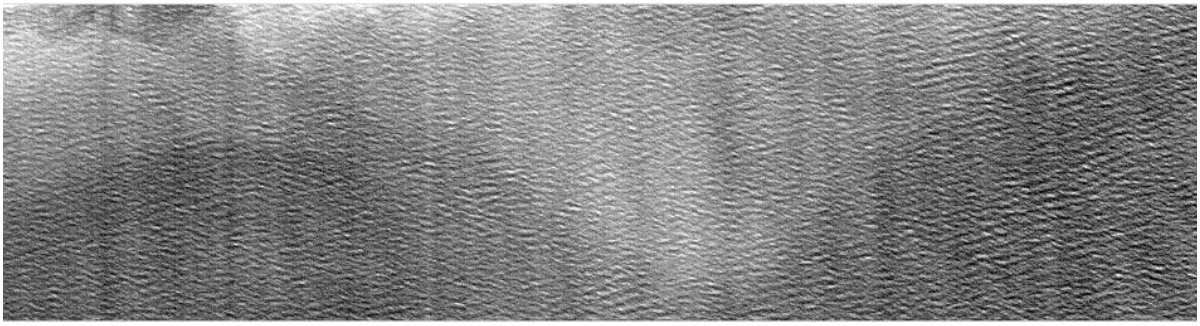

**Figure 7-26 VNIR band 7 over water, L1Bdestriped, non-lin. stretch**

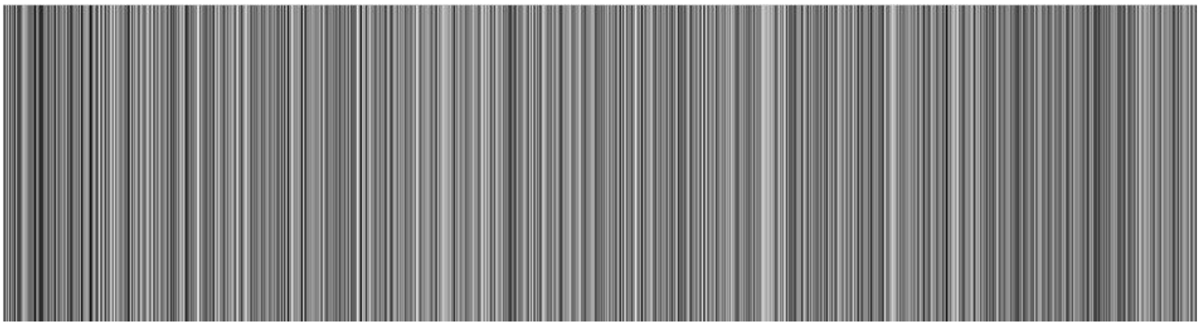

**Figure 7-27 VNIR band 7 over water, abs. difference of L1Bint and L1Bdestribed, non-lin. stretch**

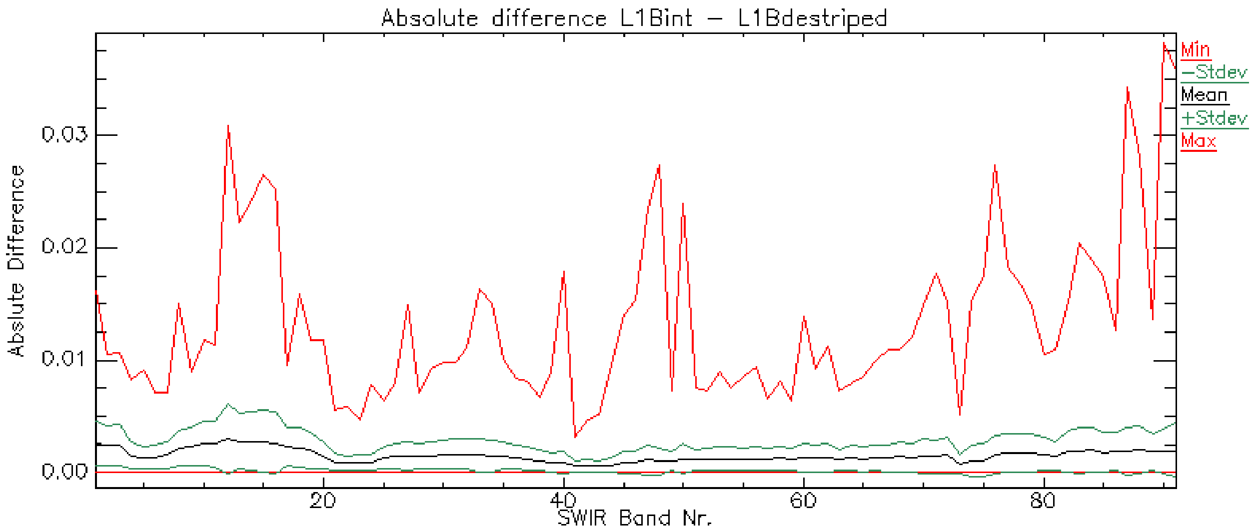


**Figure 7-28 SWIR image statistics of the absolute difference between L1Bint and L1Bdestriped**

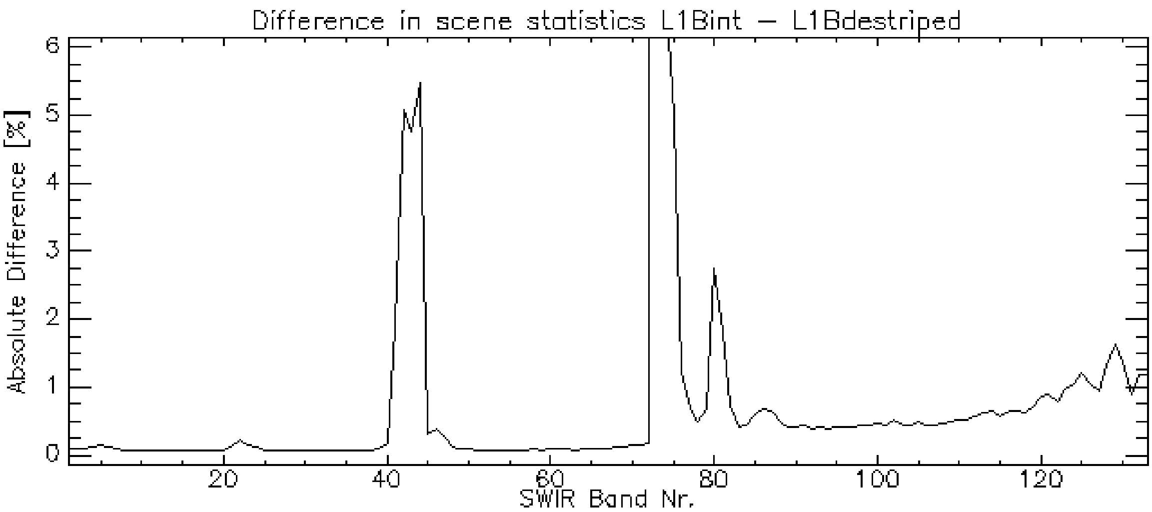


**Figure 7-29 SWIR image statistics of the relative difference between L1Bint and L1Bdestriped**

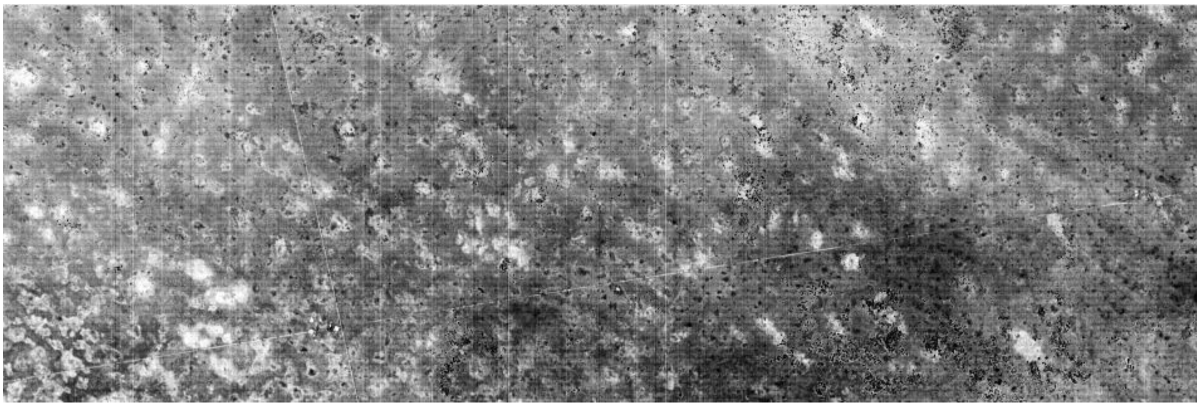

**Figure 7-30 SWIR band 82 over land, L1Bint, non-lin. stretch**

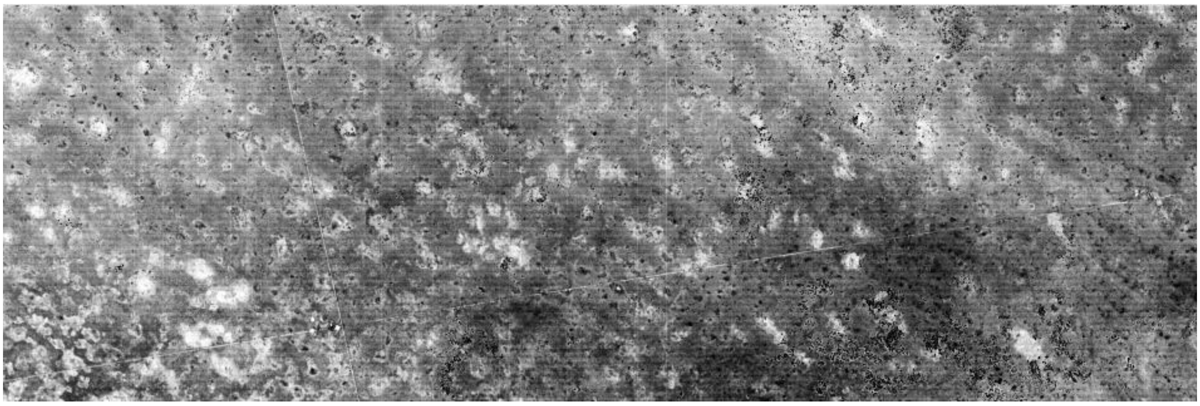

**Figure 7-31 SWIR band 82 over land, L1Bdestriped, non-lin. stretch**

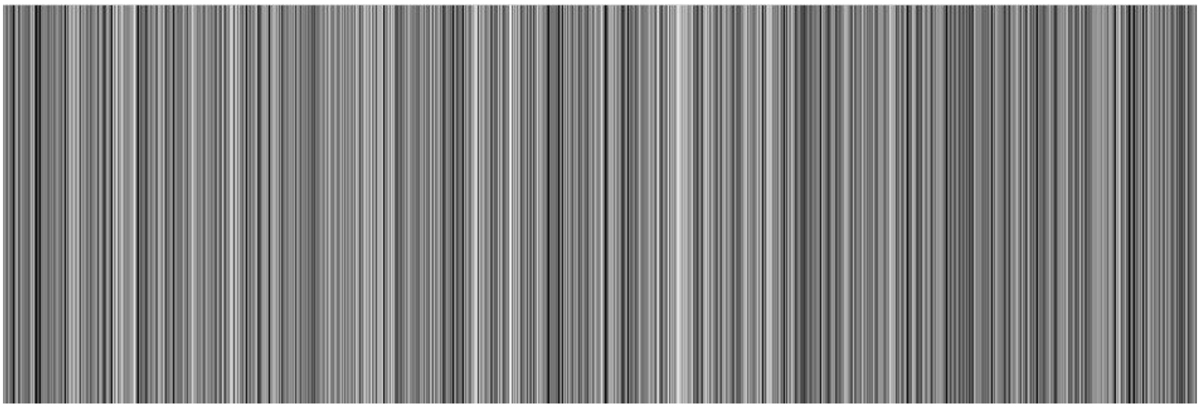

**Figure 7-32 SWIR band 82 over land, abs. difference of L1Bint and L1Bdestribed, non-lin. stretch**

## 2. Image Artefacts: VNIR Fringing / Etaloning

Fringing (also known as etaloning) is an expected effect of the VNIR CMOS detector. Fringing is a mixed spectral and radiometric effect. The Level 1B product shows an along-track low frequency variation which is constant across all frames (see Figure 7-33 and Figure 7-34) and does not appear in the lower bands nor in the SWIR (Figure 7-35). These fluctuations also appear in the across-track profiles shown in Figure 7-36, causing a wave pattern towards the edges of the image for the VNIR bands at longer wavelengths. Note that due to the very homogeneous observation site and the stacked plots in Figure 7-36 the fringing is highlighted, and usually shows less impact on observations. Based on results from the DESIS mission which features a VNIR CMOS detector from the same waver (but with differences regarding shutter and read-out wavelengths), the stability and the magnitude of the fringing strongly depends on the observation, not allowing for a generally valid estimation of the magnitude.

**Figure 7-33 Fringing of the VNIR, illustrated by non-linear image stretch over homogeneous PICS**

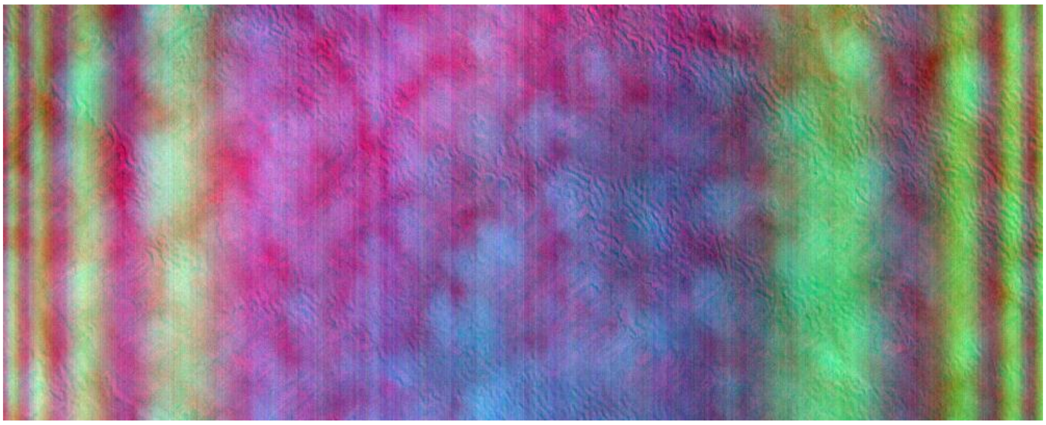

**Figure 7-34 Fringing of the VNIR, Principal Component-transformed data**

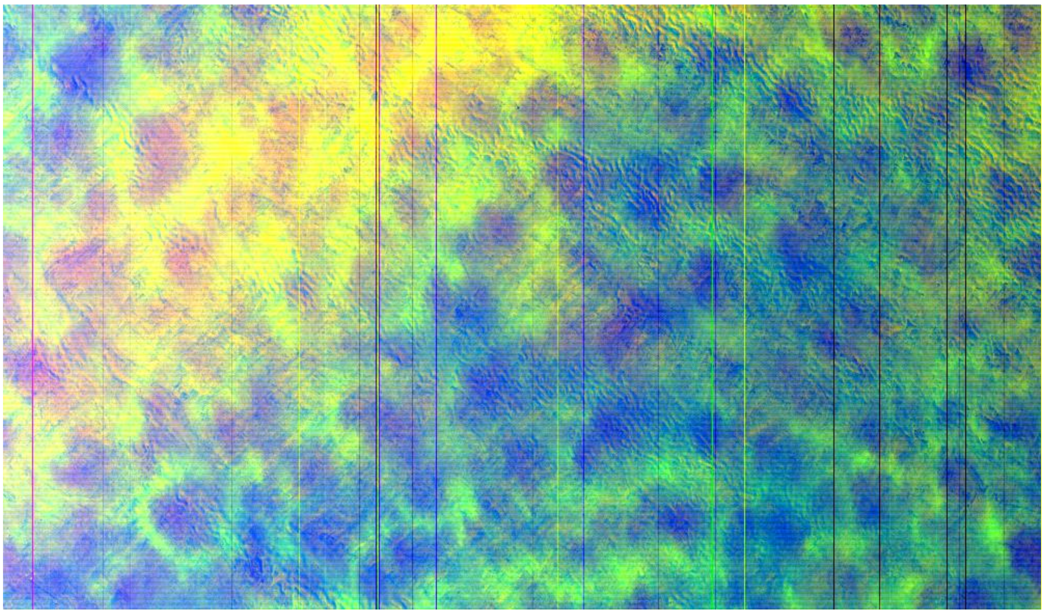

**Figure 7-35 Principal Component-transformed data of the SWIR (no fringing) for comparison**

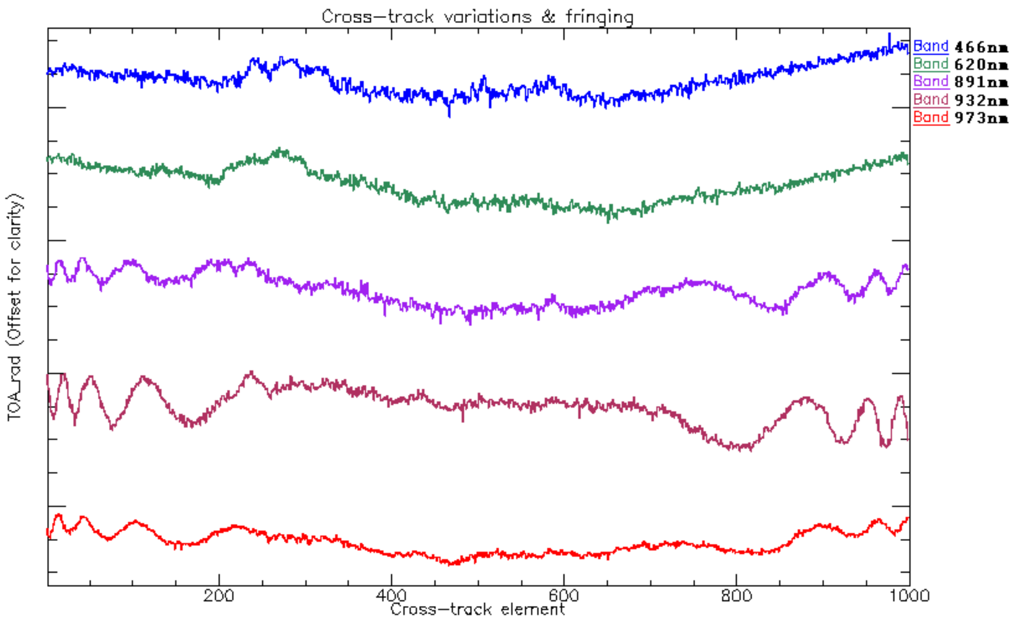


**Figure 7-36 Across-track profiles for various VNIR bands, fringing influence increases towards bands at longer wavelengths**

### 3. Image Artefacts: Micro-Vibration Effects on the SWIR

An additional effect on the SWIR is along-track striping due to SWIR-A compressor micro-vibration harmonics, resulting in a regular striping pattern in along-track direction, as highlighted by a principal component transformation shown in Figure 7-37. As shown in Figure 7-38, the magnitude of the along-track striping is relatively small and cyclic, with a relative magnitude below approx. 1% (which also includes the influence of the natural heterogeneity of the site).

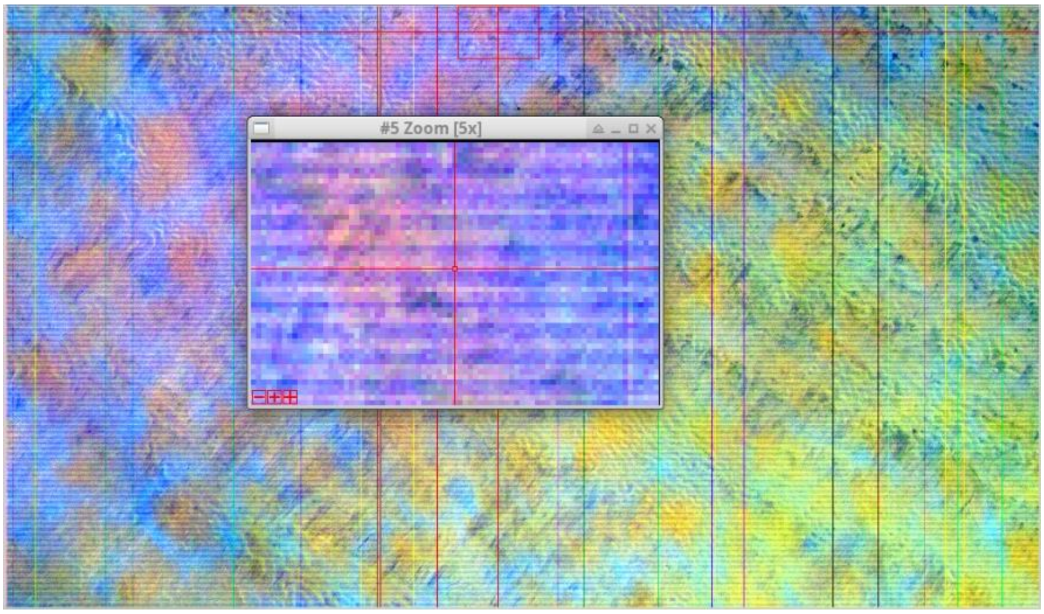


**Figure 7-37 Principal Component Analysis (PCA) highlighting along-track striping**

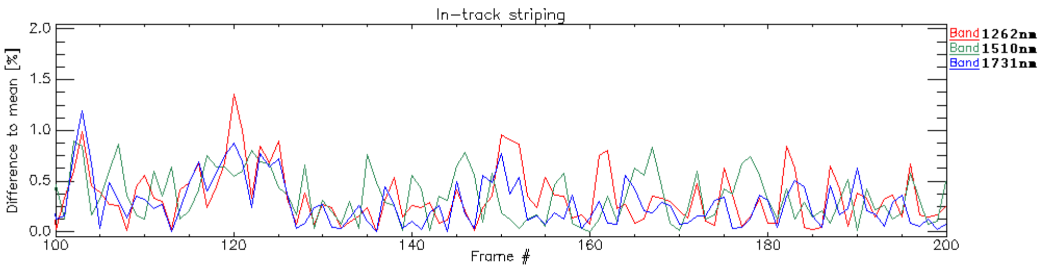


Values in [%] relative to the average.

**Figure 7-38 Along-track profiles in Level 1B TOA radiances for 100 frames**

To summarize, concerning Level 1B:

- Spectral stability and smile are within the requirements of the mission
- Absolute and relative radiometric calibrations are within the requirements of the mission
- Striping and other image artefacts are within the requirements of the mission
- The three identified anomalies, i.e. striping and fixed pattern noise, VNIR fringing / etaloning, SWIR micro-vibration effects, and methods for their correction are under further investigation

### 7.6.3 Level 1C

This report covers the timeframe between 01.01.2023 and 31.03.2023. A geometric calibration was performed beginning of February 2023 and the resulting calibration table is valid since 11.02.2023. A processor update (V01.02.01) was installed on 27.03.2023 resulting in a new geometric calibration table used after this date. Due to an outage of the satellite from 13.12.2022 to 07.02.2023, no data were acquired during this time.

In the timeframe of this report, 615 datatakes have been acquired. In 319 of those datatakes (~52%), enough GCPs and ICPs were found to perform a geometric accuracy assessment. The datatakes without enough GCPs were not assessed quantitatively, but a random subset of them was inspected visually. The vast majority of those datatakes was either almost fully covered with clouds or showing only water, desert or rain forest. The behavior is thus as expected.
The assessment of the RMSE values in the metadata is shown below in Figure 7-39.

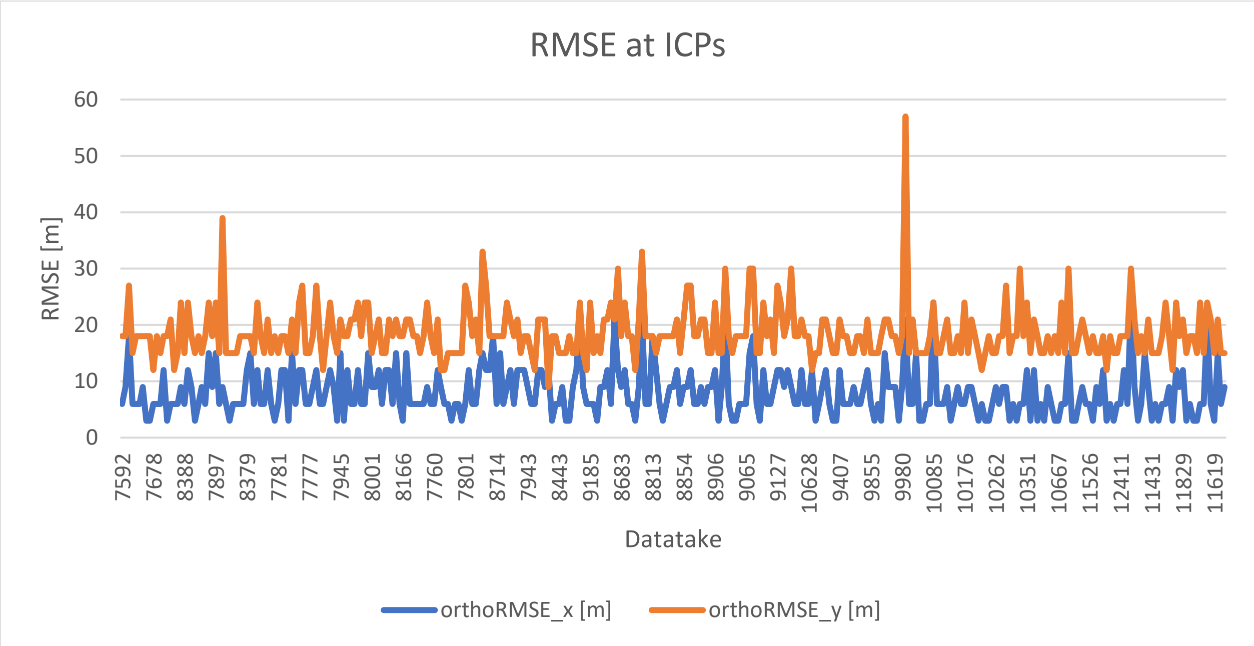


**Figure 7-39 Assessment of RMSE values, calculated based on found ICPs, for all datatakes**

In x-direction, no datatake (~0.0%) has an RMSE value above 30 m (1 GSD), whereas in y-direction, 4 datatakes (~1.2%) are above this threshold. The mean values are 7.98 m in x-direction and 18.57 m in y direction. This shows a very high geolocation accuracy for the datatakes where matching was possible. The requirement GRD-PCV-0155 is thus fulfilled.

However, it is obvious that the RMSE values in y-direction are approximately twice as large as in x-direction. After a very thorough investigation, the reason for this was identified: The speed of light correction is turned on during orthorectification. However, it is already implicitly included in the estimated boresight angles and is thus applied twice. In a test with three datatakes, the RMSE in x-direction was basically the same, but in y-direction was improved to be in the same order as in the x-direction. That means, once this change is incorporated in the processor with the next processor update (currently planned for beginning of May 2023), the RMSE values are expected to be around 8-9 m in both x- and y-direction. Newly ordered (after the planned processor update) L1C/L2A products will already include this change, however, in the metadata the RMSE values will remain the same until a L0 reprocessing is done (currently planned to start in May 2023). In the next report, this will be further investigated.

The average boresight angles, which can be interpreted as the correction and thus the error of the scene if no GCPs could have been found, corresponds to approximately 30 m in x direction and -25 m in y direction on ground with a standard deviation of approximately 23 m and 22 m in x- and y direction respectively. It is reasonable to assume that the scenes where no GCPs could be found are in the same accuracy range and thus well within the requirement of 100 m (GRD-PCV-0150).

Note that the x and y direction mentioned in this report are not in the image coordinate system but in UTM, as the evaluation is done on L1C products.

#### 7.6.3.1 Geometric accuracy

EnMAP L1C products are matched against a reference image (Sentinel-2 data, if not stated otherwise) by using image matching techniques to assess the geometric accuracy. At the obtained checkpoints, statistics are calculated to provide mean and RMSE values for each scene.

The requirement GRD-PCV-0155 shall be fulfilled:

*The geolocation accuracy at nadir look direction of level 1C and 2A products shall be better than 1 GSD (1 sigma) in each direction with respect to reference images provided that reference images are available and sufficient similarity.*

Note that the obtained accuracy in the analysis is always w.r.t. the reference image.
This report covers EnMAP data from 01.01.2023 to 31.03.2023. A random sample of 292 L1C tiles was selected based on visual inspection of the catalogue quicklooks (e.g. to avoid cloudy images).

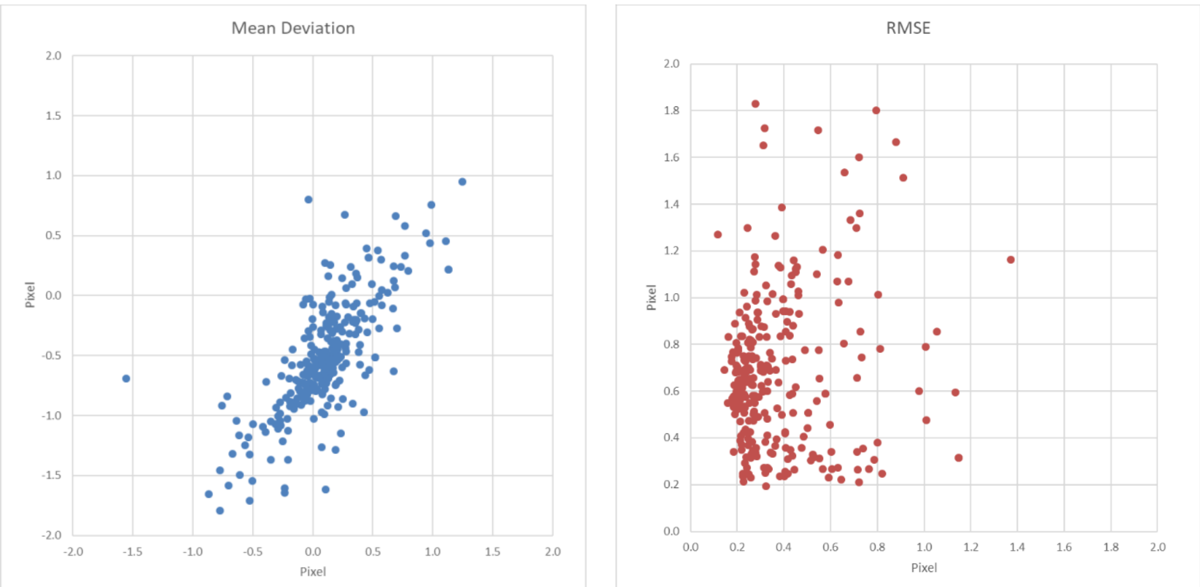


**Figure 7-40** Mean deviation of EnMAP L1C products in pixel (left). RMSE value for EnMAP L1C products in pixel (right)

The data show, that the co-registration is in the order of 0.15 pixel in both in x and y direction for data processed with the geometric calibration table V01.01.00 with validity date starting on 11.02.2023. This is already within the requirement. Based on only 8 tiles processed with the processor version 01.02.00 and the corresponding geometric calibration table V01.02.00, the co-registration seems to be further improved to around 0.1 pixel in x and y direction respectively. Note that the theoretical accuracy of the used matching algorithm is 0.1 pixel, and as can be seen in the RMSE values, still some mismatches were not removed by the blunder detection techniques that were applied.

#### 7.6.3.2 Co-registration accuracy

In this chapter, the co-registration accuracy is checked against the Space Segment requirement SRDS-PIM-0050 and later waivers on this requirement (EN-KT-RFW-003).
For the assessment of co-registration accuracy, the SWIR data of EnMAP L1C products are matched against the corresponding VNIR data.
This report covers EnMAP data from 01.01.2023 to 31.03.2023. The orange points mark the tiles processed with version 01.02.00 of both the processor and the geometric calibration table. The update was done on 27.03.2023.


**Figure 7-41** Mean deviation in pixel between VNIR and SWIR data of EnMAP L1C products (left). RMSE in pixel between VNIR and SWIR data of EnMAP L1C Products (right)

### 7.6.4 Level 2A

**Atmospheric correction over land**

Within the time interval between 2023-01-01 and 2023-03-31, an interactive in-depth analysis has been conducted for the following scenes (Table 7-24):

| datatakeID | tileId | date | location | L2A option | cirrus and haze removal | Overall Quality |
|---|---|---|---|---|---|---|
| 3986 | 21 | 28.09.2022 | Windsbach, Germany | Land_Mode | No | 0 |
| 9888 | 1 | 05.03.2023 | Nanjanagudu, India | Land_Mode | No | 0 |
| 9888 | 1 | 05.03.2023 | Nanjanagudu, India | Combined | No | 0 |
| 8775 | 1 | 04.03.2023 | Donau, Wien, Austria | Combined | No | 0 |
| 1849 | 14 | 20.07.2022 | Bavarian Forest, Germany | Land_Mode | Cirrus_and_Haze | 2 |
| 1849 | 14 | 20.07.2022 | Bavarian Forest, Germany | Land_Mode | No | 2 |
| 7593 | 5 | 07.02.2023 | Dar es Salam, Tansania | Combined | No | 0 |

**Table 7-24** **Inspected L2A scenes**

| datatakeID | cloudCover | cirrusCover | hazeCover | snowCover | status | processor version | Quality evaluation |
|---|---|---|---|---|---|---|---|
| 3986 | 66 | 53 | 1 | 4 | REDUCED | 01.02.00 | Nominal |
| 9888 | 0 | 0 | 1 | 0 | REDUCED | 01.02.00 | Nominal |
| 9888 | 0 | 0 | 1 | 0 | REDUCED | 01.01.11 | Nominal |
| 8775 | 0 | 0 | 1 | 0 | REDUCED | 01.01.11 | Nominal |
| 1849 | 0 | 16 | 2 | 0 | REDUCED | 01.01.11 | Nominal |
| 1849 | 0 | 16 | 2 | 0 | REDUCED | 01.01.11 | Nominal |
| 7593 | 64 | 17 | 1 | 24 | REDUCED | 01.01.11 | Nominal |

**Table 7-25** **Inspected L2A scenes (more details)**

Two different processor versions, different L2A processing options and different scene quality ratings were included. No RadCalNet sites were covered within this period. All scenes analyzed were rated as nominal.

L2A data was examined of the first data acquisitions after mission outage: Example of Dar es Salam acquired 7th of February 2023 (see Figure 7-42 and Figure 7-43 below):

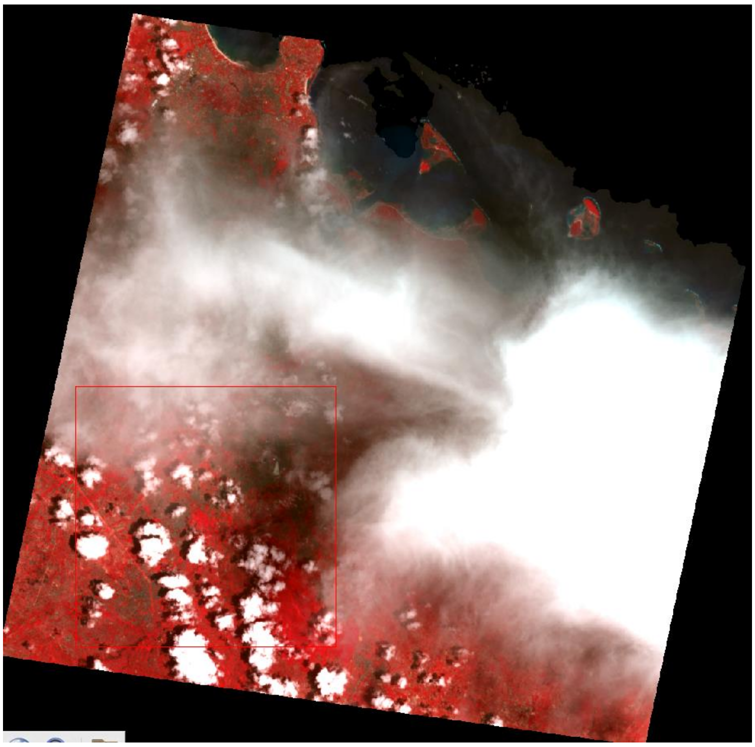

**Figure 7-42 CIR composite for DT 7593**

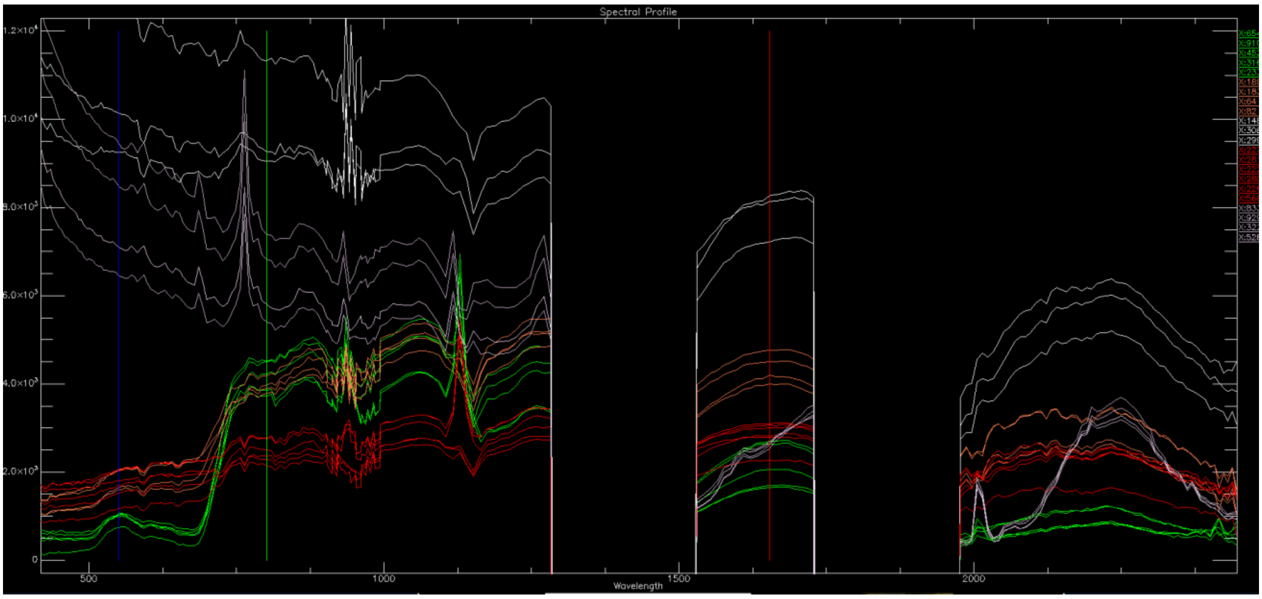


**Figure 7-43 Spectra for different surfaces: green = vegetation; sienna = dry vegetation; white = cumulus; red = settlement; grey = cirrus**

Another example of L2A data and corresponding spectra of different surfaces (DT 9888), see Figure 7-44, Figure 7-45:

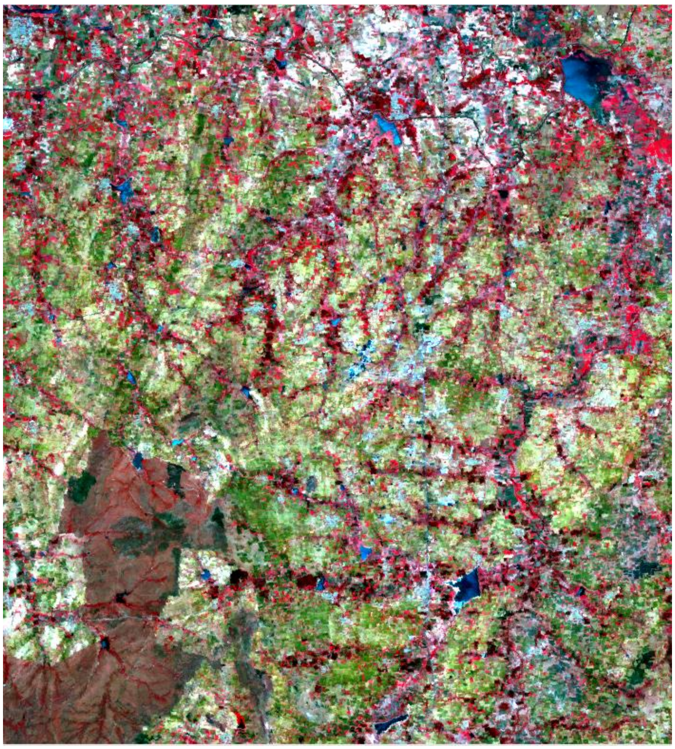

**Figure 7-44 CIR composite for DT9888**

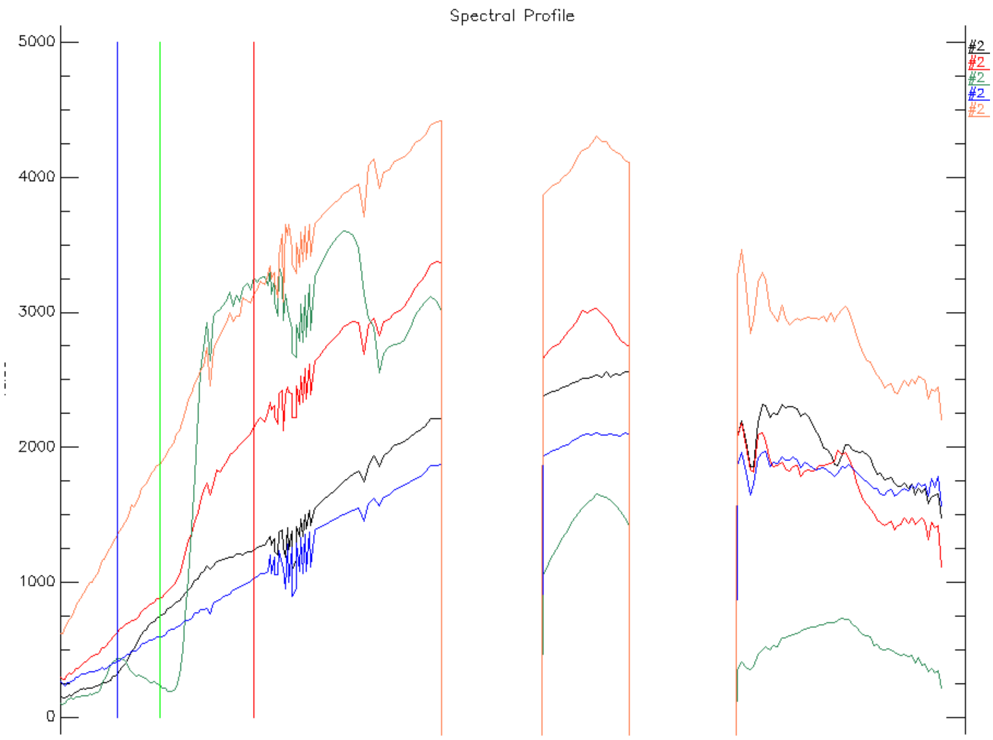


**Figure 7-45 Spectra for different surfaces**

The consistency between L2A_land and L2A_combined for DT 9888 has been verified (see Figure 7-46, Figure 7-47 and Figure 7-48 below), checking that the processing options are applied correctly.

The results correspond to the specifications: for all pixels over land, the resulting BOA_ref spectra are identical for land and combined (as is the case for the black and blue spectra in Fig. Figure 7-48), and the only differences are for water pixels, which are correctly classified as water.

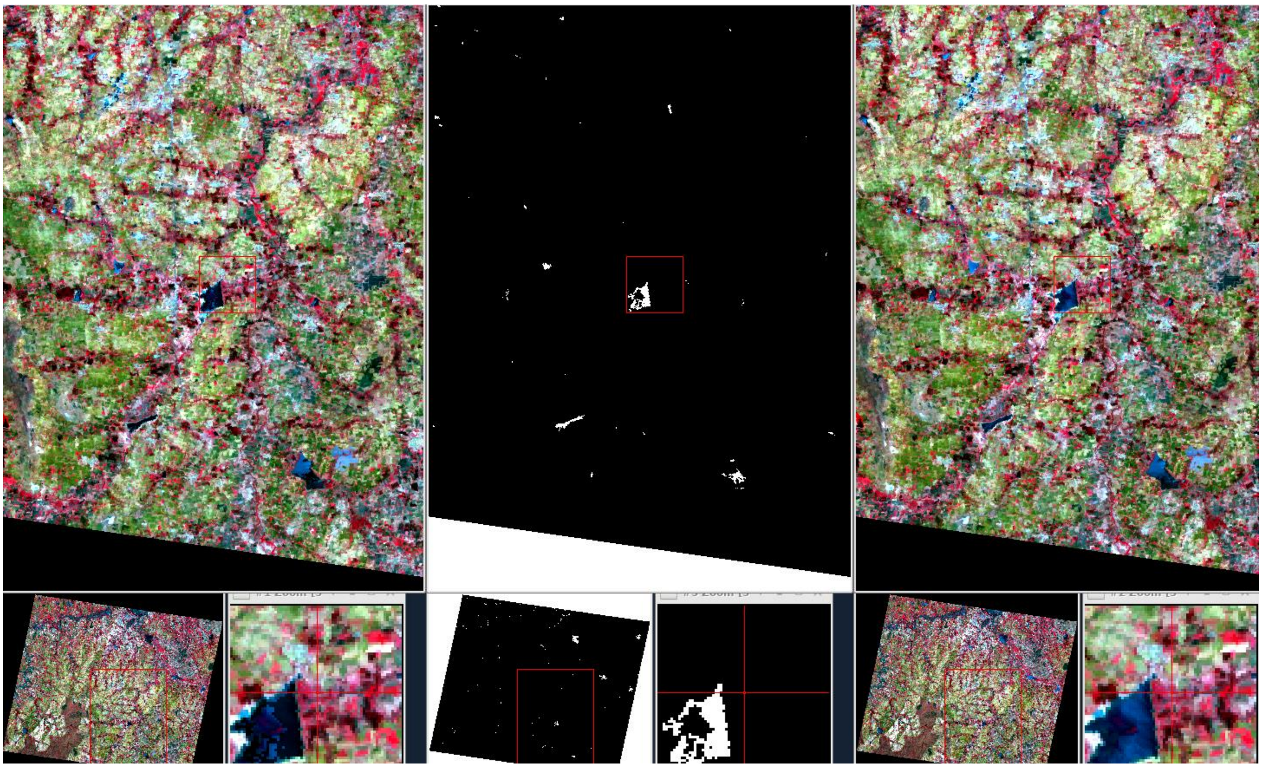

**Figure 7-46 L2A processing with combined (left) and land (right) mode plus water mask (middle)**

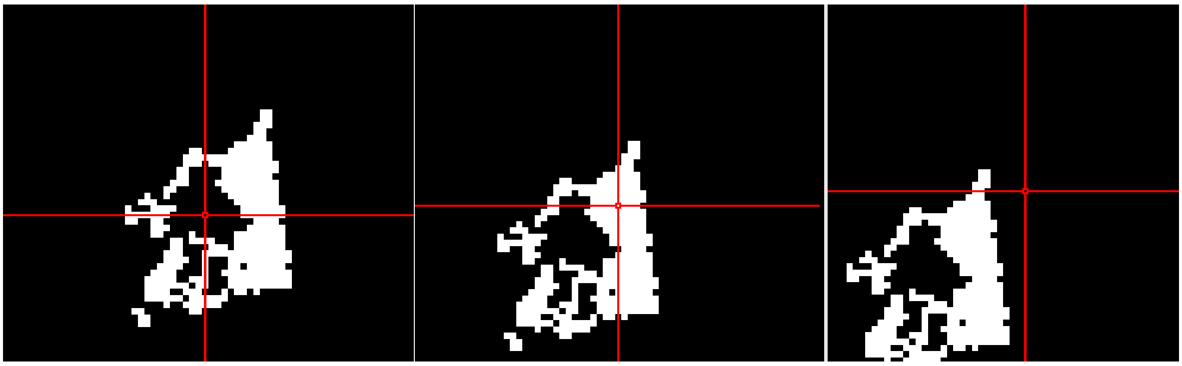

**Figure 7-47 Locations of spectra extracted for comparison**

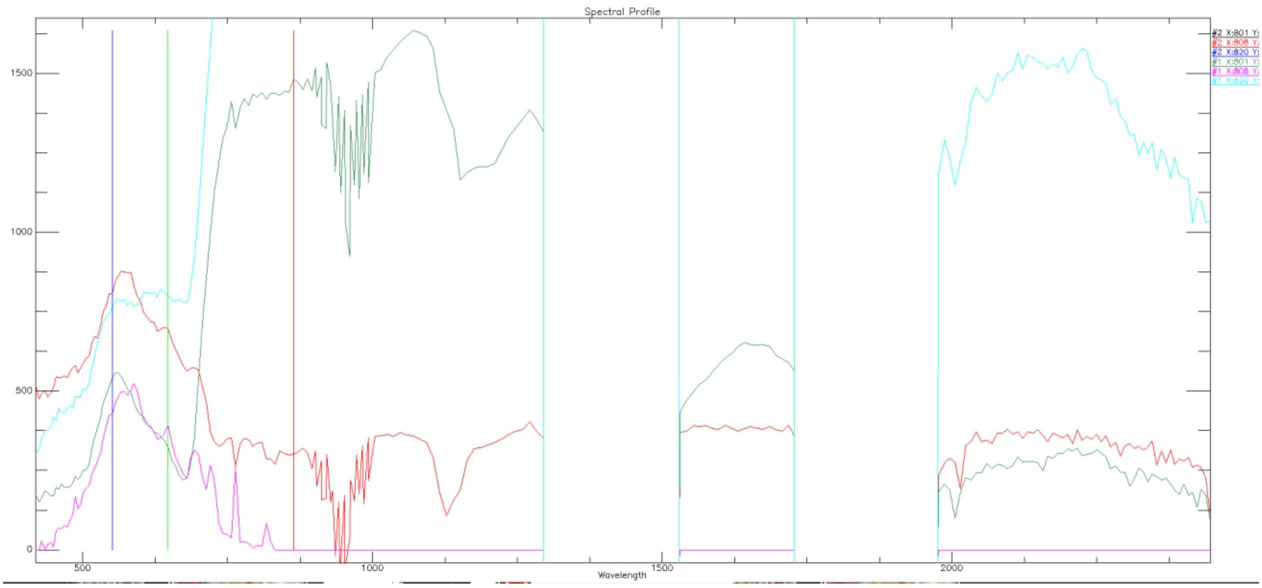


**Figure 7-48 Comparison of spectra using combined and land mode. green/black = position 1 (water masked as land); red/magenta = position 2 (water masked as water), blue/cyan = position 3 (land masked as land)**

Quality of masking:

Below figures show results of the quality masking (example DT 8775), showing a slight misclassification in the cloud / cloud shadow mask (Figure 7-49) and nominal results for the land/water masking (Figure 7-50).

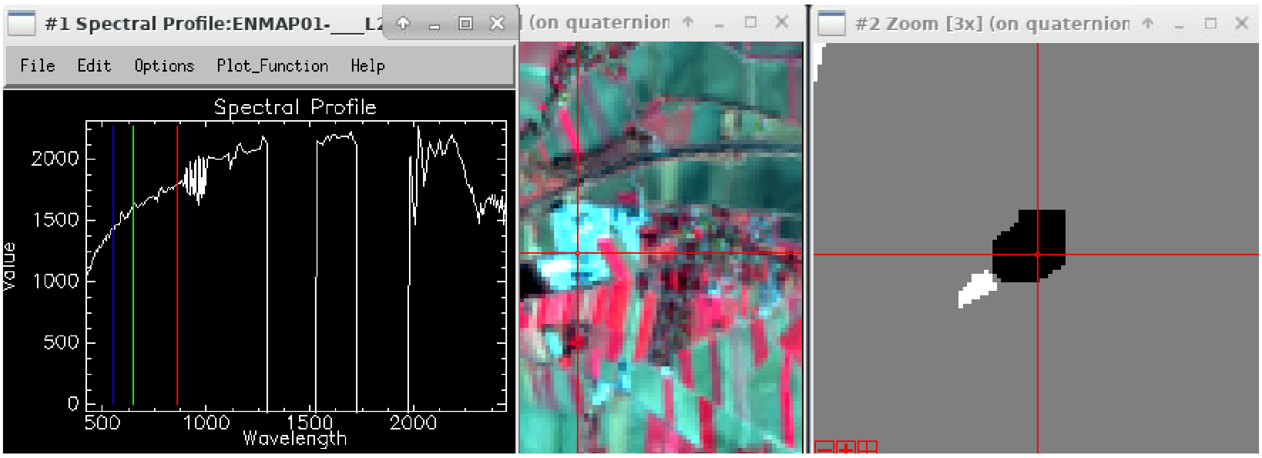


**Figure 7-49 Comparison of BOA_ref spectrum (left), CIR image (center) and cloud/shadow masking (right) for DT 8775**

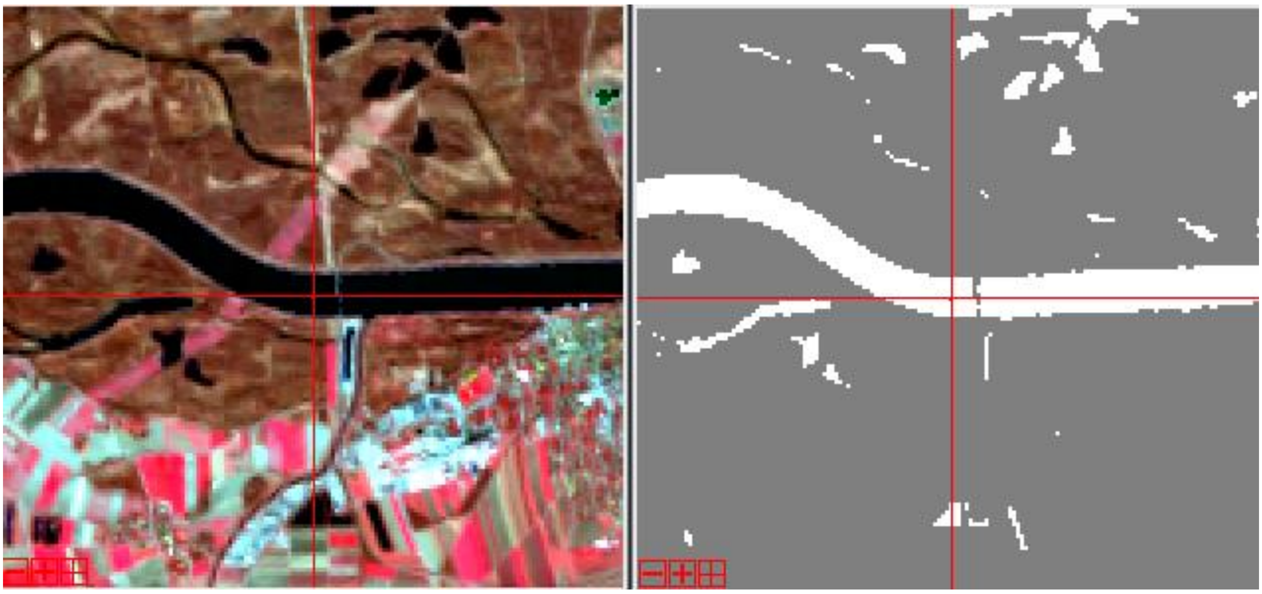

**Figure 7-50 Second example, comparison CIR image (left) and land/water masking (right) for DT 8775**

**L2A snow spectra discrepancy**

It has been observed that in some circumstances the L2A spectra over snow is overestimated at wavelengths below 750 nm. This issue is caused by a confusion of the cloud and snow masks and it is under investigation at the moment.

**Atmospheric correction over water**

As part of the evaluation of water products done by EOMAP, the following scenes were taken into consideration and checked by EOMAP:

| Reference | Datatake ID | Processor Version | Comment |
|---|---|---|---|
| **[L2A-8]** | DT0000004713 Tile 02 | V01.02.11; | Masking (Land, Water, Clouds, etc.): No issues found.<br><br>Adjacency correction: No issues found.<br><br>Low impact within the used scene: To check for future scenes, when available.<br><br>Retrieval of atmospheric properties: No issues found.<br><br>Cirrus – correction: No issues found.<br><br>Retrieval of water leaving reflectance: No issues found. |

**Conclusion:** The atmospheric correction over water works as expected. No need for further action.

# 8. External Product Validation

The activities of the external product validation during the reporting period focused on the overall data quality validation on acquisitions taken after the 1.5-month outage and the new preprocessing version 01.02.01, which introduced significant improvements regarding the overall product data quality.

### 8.1.1 General

Several EnMAP acquisition requests which ordered only a single tile did not fully cover the AOI. These circumstances identified a pointing offset in the along-track direction during the acquisition procedure. The pointing offset is under investigation now. It does not influence the data product's absolute or relative geometric accuracy but leads to missing targets or only partial coverage. A workaround for the user is to request the acquisition so that at least one tile is acquired (acquisition circle radius > 20 km) before and after the AOI.

### 8.1.2 Level 1B

Level 1B products were validated in detail and in-depth during the reporting period to validate the data quality after the outtake and the major preprocessing update:

- TOA Radiance
- Spatially coherent radiometric miscalibration (striping artifacts)
- Signal-to-Noise Ratio (SNR)
- Keystone

Several matchups with in-situ measurements were generated to validate the TOA radiance quality. The focus was on snow sites and the southern hemisphere. The overall good TOA data quality was confirmed by these matchups. Abnormalities or changes after the outtake were not detected.

The spatially-coherent radiometric striping artifacts and undulations in the VNIR and SWIR across-track direction have been validated in detail. Significant improvements were acknowledged after implementing the across-track de-striping algorithm (developed in a joint investigation by GFZ and DLR. For both VNIR and SWIR, the spatially-coherent radiometric striping was significantly suppressed over the whole wavelength domain without losing spectral consistency. Residual low-frequent across-track undulations do not violate the mission requirements of <5% misregistration. Nevertheless, in the course of the operational phase, this issue should be addressed. The well-known along-track artifacts detected in SWIR wavelength domains with a vital gradient/feature still need to be resolved. Although the radiometric misregistrations are very small and thus far below the requirements of < 5 %, a correction should be integrated in the future since the artifacts influence the thematic products of the user and the quantitative determination.

Regarding the SNR, no significant changes have been recognized after the outtake, and the mission requirements (VNIR > 343:1 (@495 nm & SSD 4.7 nm) and SWIR > 137:1 (@2200 nm & SSD 8.4 nm) for L(TOA) reference of 30% reflective target) are still fulfilled.

No significant changes were found in the VNIR and SWIR Keystone either.

### 8.1.3 Level 1C

Level 1C products have been validated regarding:

- VNIR-to-SWIR spatial co-registration
- Absolute spatial accuracy

The tiles processed and acquired after a major geometric update achieve a VNIR-to-SWIR spatial co-registration of RMSE ~5.7, which is a welcome improvement. Thus they are well inside the mission requirements of < 30 % of a pixel.

No significant changes have been recognized for the absolute spatial accuracy validation, and the mission requirements are still fulfilled.

### 8.1.4 Level 2A

During the reporting period, L2A land and water products were investigated in-depth to validate the data quality after the outtake and the major preprocessing update. Only a few usable in-situ matchups could be generated based on which the general L2A data quality was validated.

**Land**

**As for the L1B validation,** the focus was on snow sites and the southern hemisphere. Several matchups confirmed the fulfillment of mission requirements for BOA reflectance. However, an issue with the misclassification of cirrus clouds and their correction was identified for tiles with snow surfaces. This issue will be improved and fixed in one of the upcoming processor updates.

**Water**

The L2A normalized water leaving reflectance was also investigated and was well inside the mission requirements.

### 8.1.5 Summary of External Product Validation

During the reporting period, the focus was on acquisitions taken after the 1.5-month duration outtake and critical validation scenarios and parameters that were potentially influenced by the release of the new preprocessing version > 01.02.01. Serious non-compliance with the mission requirements has not been indicated for the reporting period. Critical parameters like the VNIR-to-SWIR co-registration have been significantly improved and are now well inside the mission requirements.

# 9. Others

No EnMAP presentations during international conferences during the reporting period.